Review

The State of Critical and Strategic Metals Recovery and the Role of Nuclear Techniques in the Separation Technologies Development: Review

Nelson R. Kiprono [ID], Tomasz Smolinski [ID], Marcin Rogowski and Andrzej G. Chmielewski *[ID]

Institute of Nuclear Chemistry and Technology, 03-195 Warsaw, Poland
* Correspondence: a.chmielewski@ichtj.waw.pl; Tel.: +48-22-504-1205

Abstract: The extraction of useful minerals or geological materials from the Earth's crust, most typically from various sources, is crucial to a country's development and progress. Mineral-rich countries use these resources to transform their economies and propel them toward long-term prosperity. There is an urgent need for the world to increase mineral exploration efforts, improve the recycling of important metal-containing resources, and extract them using upgraded hydrometallurgical procedures with high recovery efficiency. This review paper highlights the importance of strategic and critical metals in the economy and the role of nuclear techniques in the analysis, process optimization, and remediation of metals using solvent extraction, adsorption, and chromatographic resins. Radiotracer analysis, X-Ray Fluorescence spectrometry (XRF), Neutron Activation Analysis (NAA), and X-Ray Diffraction (XRD) are appropriate for improving laboratory-based hydrometallurgical processes, with future technical and economic benefits. The development and installation of novel instruments to provide the real-time control of mining and mineral processing plants for improved control have the potential to aid in the recovery of a broad range of metals.

Keywords: mining; metals; hydrometallurgy; leaching; extraction; nuclear techniques; radiotracer

1. Introduction

Mining is the recovery of geological materials or beneficial minerals from the Earth's crust, usually from the lode, orebody, placer deposit, seam, or reef. Mineral exploration and mining play a vital role in a country's growth and progress [1]. Countries endowed with minerals use these resources to transform their economies towards a path of sustainable development. For instance, South Africa, Australia, Canada, and Ghana, among others, have developed due to their vast mineral resources. Other nations that have depended on the exploration and extraction of minerals for their economic development are Canada, Sweden, and the U.S.A. [2]. The exploration and extraction of minerals play a very important role for the medium-size economies such as Poland, which ranks as the E.U.'s number one producer of hard coal, coke, Cu concentrates, Ag, and He. Furthermore, it is second in refined Cu, S, and soda ash, and third in lignite, Zn, and Pb concentrate, Cd, and Se [3]. In developing nations, especially in Africa, the mining sector is expected to be the driving force for economic development. These African countries include South Africa, Ghana, the DRC, and Mali, among others.

The need for metals and minerals is due to rise due to the new infrastructure expansion in developing countries, population growth, rapid urbanization, the transition to new energy technologies, and the widespread utilization of electronic gadgets internationally [4]. The demand for crucial metals has sharply increased and will continue to increase due to robust economic expansion, and the realization of an effective supply might be challenging [5] because of the need to extract ores at deep depths, with minimal concentrations and complex mineralization. It was recently predicted that the demand for metals and minerals would increase from 9722 million tons in 2013 to 11,238 by the year 2018, a cumulative

annual growth of 2.9% [4]. According to a new World Bank Group analysis, the output of minerals such as graphite, Li, and Co may grow by roughly 500% by 2050 to fulfil the rising demand for the production of renewable energy technologies [6]. It is estimated that about 3 billion tons of metals and minerals metals will be needed in the production of geothermal power, solar, wind, and energy storage technologies in order to limit the global increase in temperature to 1.5 to 2 °C [6]. The amount of minerals and mineral reserves in first world countries has reduced gradually, which has led to massive investments in mining and exploration sectors in developing nations, primarily in Africa, Latin America, and parts of Asia. Therefore, it is crucial to improve the metal recovery processes. This paper seeks to underscore the existing critical and strategic metals, their status, and the position of Neutron Activation Analysis (NAA), X-Ray Fluorescence Spectrometry (XRF), X-Ray Diffraction spectrometry (XRD), and radiotracers in the analysis, optimization, and remediation of metals using solvent extraction, adsorption, and chromatographic resins.

1.1. Critical and Strategic Metals

Since the Industrial Revolution, there has been a dramatic upsurge in the utilization of energy resources globally, primarily fossil fuels. The World Energy Outlook indicates that the total energy requirement is projected to rise by 60% in the next twenty-five years in the regions such as the U.S.A. [7]. The global energy industry is anticipated to steadily move toward renewable energy sources in the coming few decades [8]. Renewable energy systems such as hydroelectric, photovoltaic, and wind power will perform an essential role in meeting future global demands, with the estimated growth in electricity being projected to be 150% from 2010 to 2050. To address climate change, promote competition and sustainability, and enhance energy security and supply in the E.U. economy, creating a low-carbon economy is the key policy priority. Therefore, adopting low-carbon energy technologies is central to this transition [9]. Moving toward low-carbon technologies globally will result in a significant rise in the requirement for critical metals [8]. Indeed, critical metals demand is soaring as millions of people embrace the modern lifestyle [10]. Unfortunately, the transition from a fossil-based economy to a non-fossil-based economy may be hampered by the reduction in metals required by renewable energy-based innovations [11].

1.2. Critical Metals

Metals can be categorized as critical metals if they are scarce geologically, subject to possible supply limitations, costly, and required for an economically crucial drive where substitution is hard [12], as shown in Figure 1. The critical metals are the ones essential for a green economy and scarce geologically [8]. Such metals are important because of their unique or special properties [13]. Of these properties, the prospective for supply limitations seems to be foremost. Unlike in the Medieval Era, nearly every natural element in the periodic table is now required to manufacture a wide variety of goods for society. Most of the critical metals were ignored 50 to 60 years ago and discarded as mine wastes [14].

The geologically rare but critical metals include Ge, In, Ga, Ta, Se, Sn, Te, and some Rare-Earth Elements (REEs) [13]. The term REEs refers to the seventeen elements in the periodic table, i.e., Y, Sc, La, Ce, Eu, Pm, Pr, Sm, Nd, Gd, Ho, Tb, Tm, Er, Dy, Yb, and Lu. La, Pr, Ce, Pm, and Nd are classified as Light REEs with lower atomic weight, while Sm, Eu, Gd, Tb, Dy, Ho, Er, Tm, Yb, and Lu are categorized as Heavy REEs due to their high atomic weight [15]. Sc and Y are also classified as REEs because they occur in similar ore deposits as lanthanides with the exhibition of the same chemical properties [16,17].

Figure 1. Periodic table showing different types of elements and their economic status based on [14].

The U.S. and Europe are seriously challenged by the prospective scarcity of critical resources, which might have significant economic implications [18,19]. The European Union (E.U.) listed 20 critical raw materials encompassing industrial minerals, bulk materials, REEs, and Platinum Group Metals (PGMs) to transition to a green and circular economy. PGMs entail six elements: Pd, Pt, Ru, Rh, Os, and Ir. These critical metals have high heat resistance, high melting points, unique catalytic characteristics, and high corrosion resistance, which define their industrial applications [20]. Furthermore, the E.U. revised the list of key raw materials in 2017 to incorporate the following metals: Sb, Bi, Co, Ga, Be, In, HREEs, LREEs, Sc, PGMs, Si, V, Hf, W, Mg, Nb and Ta [12]. Such critical raw materials lists are updated every three years, with the first one published in 2011, which comprised 14 CRMs, and the latest one documented in 2020, which comprised 30 CRMs [21]. The CRMs that were recently deemed essential for the E.U. exceeded the following criteria: an EI index lower limit value of 2.8 points and an SR parameter lower limit value of 1.0 points [21]. These elements are critical in realizing a circular economy, in which the value of resources and products is maintained as much as feasibly possible in the economy, while producing minimal waste. Such moves are vital to the E.U.'s efforts to create a sustainable, resource-efficient, low-carbon, and competitive economy [12]. The U.S identified REEs such as Dy, Y, Tb, Nd, and Eu as critical metals in developing clean energy-based technologies [18]. The prospects for thin-film photovoltaic modules for solar energy, such as cadmium telluride, Cu indium diselenide, thin silicon, or gallium-arsenide, will demand one or more combinations of critical metals [8,13].

REEs such as Gd, Sm, Dy, and Eu have large-capture cross-sections for thermal neutrons, which allows them to absorb a huge number of neutrons per unit area. Such properties make them crucial in the nuclear industry in the design of control rods that regulate the working of nuclear reactors by turning off and on their system when necessary. Additionally, to raise the temperature of the reactor, the mechanical properties and melting point of the fuel must be raised, which requires the metallic alloys of some REEs for the fuel rich in lanthanide (Y) and actinides. La or other REEs can act as stabilizers [22].

1.3. Strategic Metals

Strategic metals are another class of metals that are very vital in the future and current world's technologies. Strategic metals are those materials needed for important purposes in a war situation and whose acquisition in acceptable quantities, quality, and timing is substantially unpredictable for any cause to necessitate advance planning for their supply [23,24]. Nonetheless, a metal may be considered strategic for a specific firm or industries such as automotive, aerospace, renewable energies, nuclear, electronics, and information Communication technology, among other sectors of the economy. The strategic metals vary from one region to another. For instance, the UK Government classified the following minerals as strategic: Sb, Be, Cr, Co, Ga, Ge, Au, Hf, In, Li, Mg, Ni, Nb, PGM, Re, REEs, Ta, Ti, W, and V. On the other hand, the European Commission 2014 listed the following as critical raw materials: Sb, Ga, Ge, Be, Cr, Co, Borates, fluorite, graphite, In, magnesite, Nb, Mg, PGMs, phosphate (PO_4^3), REEs, Si, and W. For the Russian Federation, the strategic mineral minerals were U, Mn, CRMs, Ti, bauxite, Cu, Ni, Pb, Mo, Co, Sc, Be, Sb, Sn, Zr, Ta, Li, Au, Ag, P.G.M.s W, Nb, Ge, Re, HREE, and diamonds [23].

Metal such as rhenium (Re) is essential in the superalloy sector, which uses 80% of Re. Re also acts as an additive to Mo- and W-based alloys, as Re–Mo alloys in superconductors at 10 K, and as filaments for mass spectrographs and ion gauges (Mishra et al., 2012). Another example is Li, which is vital for extensive application in the future generation in sectors such as cordless devices, electric mobility, and energy storage. The most important compounds of Li for generating tradable products are Li_2CO_3 and LiOH, with overall amounts of 46% and 19%, respectively, in 2015 [25]. A study was conducted on the minor and strategic metals in the automobile industry, where products such as Ford Focus, Ford Fiesta, and Ford Fusion have been witnessed recently [26]. The study reported the following as strategic metals facilitating the production of automobiles: Nb, Sn, Mg, LREEs, Ag, Co, HREEs, W, Au, P.G.M.s, Mn, and Al. Although the materials are strategic in the industry, REEs are facing supply threats in different regions, such as the U.S.A. and Japan, due to high demand. That could be attributed to the acceleration of the technological revolution and commercialization of products and industries such as solar photovoltaic, wind power generation, additive manufacturing, and electric vehicles [27].

Generally, REEs forms a very important basis for the strategic metals meant for shaping the future generation in the context of the green economy. Although REEs are widely distributed globally, 90% of them globally are mined in China, with China having ownership of 23% of the total worldwide reserves. However, intense REEs mining in China has led to a decrease in such metals from 75% in the 1970s to 23% in 2011 [16].

Strategic metals are very vital in major industries [28]. Taking into consideration ammunition and electronic components, among others utilized in the aeronautics sector, the critical and strategic materials are W, Cu, REEs, Ga, Nb, and Mo in the European Union. However, half of the strategic materials identified are imported from nations outside the E.U. For instance, 44% of W is being imported due to its high applicability in various sectors and low substitution capacity [29]. That means the intense recovery of such metals from the available sources should be prioritized using effective techniques such as hydrometallurgy [30,31].

1.4. Current Progress in Nuclear Technologies

Numerous fields have made extensive use of nuclear technology (sealed source, imaging technologies such as gamma scanning, radiotracer, nucleonic measurement, and Control systems) to optimize and track operations, conserve energy and resources, increase product quality, and minimize the effects on the environmental. Several commercial sectors have seen and acknowledged their advantages in terms of technical, environmental, and economic factors [32]. It has been established beyond a shadow of a doubt that nuclear techniques are useful for inspecting or troubleshooting and fixing production processes, as well as for quality control on manufacturing lines. Today, on an industrial and laboratory scale,

nuclear procedures based on either open or sealed sources have frequently been employed to offer alternatives to issues that would otherwise have been insurmountable [33].

Although the principles of radiometric measurements have not changed significantly, huge progress has been made in the development of apparatus. Moreover, new applications of techniques currently being used have been found. With the development of technology, the apparatus has been significantly miniaturized. Detectors based on diodes, the size of which is comparable to the size of a coin, can now be used to measure ionizing radiation. Furthermore, modern devices require a small supply voltage of a few volts and a current of about tens of microamps [34]. With the development of Information Technology (IT) infrastructure, devices can often be controlled remotely or even wirelessly [35]. The sensitivity, precision, and ease of use of modern devices using ionizing radiation have also improved significantly. Attention should also be paid to neutron generators, which are increasingly used for the needs of the mining industry. These technologies allow for a simple and quick way to optimize the process by, e.g., sorting the ore according to the content of various metals and searching for new deposits. Hole logging technology characterizes minerals in drill core samples, which is helping the industry improve the efficiency of the processes [36]. Currently, a pulsed neutron well logging technology supports geological research. The parameters of oil saturation, porosity, and water flow can be determined by recording gamma rays or thermal neutrons, which are produced through the reaction of fast neutrons produced by a pulsed neutron source with the nuclei in the borehole [37,38]. Significant development and use of nuclear techniques have been noticed, especially in developing countries such as India, where radiotracer techniques are one of the main methods of troubleshooting in the industry [39].

Multiple-radiotracer phase velocity measurement, triple phase volume, dual-source gamma tomography for measuring two-phase volume fractions, radioactive particle tracking for estimating phase velocity, flow pattern, mixing intensity, turbulent parameters, and transmission and emission tomography for gauging dynamic phase velocity are some of the recent cutting-edge nuclear techniques that have been invented, validated, and applied in laboratory-based analysis [32]. For instance, Ru is a strategic and critical metal belonging to the Platinum Group Metals (PGMs), and therefore, its recovery/separation process is paramount. For this reason, active solvent extraction investigations with the radiotracer ^{106}Ru were recently carried out from the modelled alkaline medium in n-dodecane utilizing isodecyl alcohol (IDA) as the phase modifier and Aliquat 336 as the extractant. The recovery process was evaluated by the application of a spectrometer using a High-Purity Germanium (HPGe) detector. The same procedure was used for separation experiments using an actual waste solution containing various radionuclides such as ^{137}Cs, ^{125}Sb, and ^{90}Sr. Fourier transform infrared spectroscopy, ultraviolet visible spectrophotometry, and Raman spectroscopy were then used to detect the existence of the chemical species in both the aqueous and organic phases.

In the majority of emerging economies, these strategies are still in their infancy. Due to a variety of issues that developing nations must confront, even the most important radiotracer and sealed source approaches are still neglected. They may suffer from a lack of technical skills and knowledge, equipment constraints, a lack of radioisotope availability, stringent restrictions that are not related to genuine impacts on radiological protection, etc.

Generally, the limits of studies using XRF spectrometry carried out at synchrotron radiation sources keep expanding and are used in laboratories, giving opportunities to observe the physicochemical parameters changes in situ. That is exemplified by the nanoscale spatial resolution with near single-atom specificity for the highly successfully identified metals in nanobeam operations and robust speed 3D/2D imaging abilities. Such advancements will be led by the presently under construction 4th generation synchrotron radiation equipment, including the European Synchrotron Radiation Facility—Extremely Brilliant Source (EBS) [40]. It is becoming more common to merge remotely sensed elemental data with speciation and morphological/structural imaging using synchrotron radiation–XRF spectrometry and complementary X-ray imaging/spectroscopic methods. Concerning the

optics utilized, full-field micro-XRF spectrometry has achieved some incredibly positive progress. Low count rates, which frequently limit the maximum capabilities of full-field laboratory configurations, may be circumvented via coded apertures. Economical full-field detectors will broaden the customer base and promote the development of full-field micro-XRF spectroscopy. The advantages of this microanalytical technique over the Inductively Coupled Plasma-Mass Spectrometer (ICP-MS) in the context of short sampling times with excellent particle size resolution are becoming increasingly evident as the ambient air Total Reflection–XRF spectrometry (TXRF) technology develops. The elemental assessment of air components applying ICP-MS and TXRF spectrometry was compared [40]. For metals at levels of about 1 ng m^{-3} (Pb, Ni, and V (strategic metal)) and the readily available metals (Zn, Fe, Mn, Cu, and Cr), the elemental levels (2 to 110 ng m^{-3}) detected by the two techniques varied by 18% to 230% and 3% to 62%, respectively. For these kinds of low amounts, this was regarded as permissible. Generally, TXRF spectrometry provided sampling intervals that were less than 12 h long, with a limit of detection of roughly 10 pg m^{-3}. TXRF has also been reported recently to be crucial in the analysis of polymetallic deposits known to be the primary source of strategic metals in the global industrial and commercial sectors [41]. Some metals, such as Co, Cu, and Ni, for example, are indispensable in the fields of medicine, energy materials, semiconductors, and so on [41]. Due to the introduction of archetype/pilot TXRF technology and the accessibility of commercially available XRD configurations with energy-dispersive sensors, excellent grazing incidence XRF research in the lab is now more feasible.

The richness of chalcophile metals in Cretaceous–Paleogene boundary clays linked with the end-of-the-Cretaceous effect event that occurred 66 million years ago in Denmark was investigated using remotely sensed Synchrotron Radiation–XRF and X-ray absorption near edge structure (XANES) studies. The levels of numerous chalcophile metals, comprising Pb, Cu, and Ag coincided with that of Ir (strategic metal) indicating that these metals were delivered to the seawater by mechanisms connected to the end-of-the-Cretaceous asteroid impact [40]. The SR-XRF analysis showed that Ag and Cu were present either as trace metals in pyrite particles or as different phases rich in Cu or Ag, ranging in dimensions from 1 to 10 mm. Such information was discovered by employing radiation line 37XU at SPring-8 (Hyogo, Japan), with a confined radiation of 0.5 to 0.3 mm at 14 keV for sub mm assessments or 1.8 to 1.3 mm at 30 keV for broader analysis.

On the contrary, sophisticated XRD gives details on electron density, crystalline symmetry, roughness, and strain. Coherent scattering of the radiation by periodically spaced atoms causes dispersed radiation to generate spot patterns from single crystalline materials and ring patterns from polycrystalline materials when the beam impinges upon solids [42]. A particular crystal structure can be identified by the pattern, diffraction maxima intensities (lines or peaks), and their positions (interplanar spacing d$_{hkl}$ or Bragg angle). More than any other analytical technique, XRD was mentioned in about 100,000 articles in 2016 and 2017 combined [42]. In one of the instances, the method was used to analyze activated charcoal support that included the strategic metal Ru [42]. It was determined that the type of support and distribution affects the minimal concentration that XRD can detect.

In the past 25 years, indexing algorithms have progressed significantly; nonetheless, identifying the present lattice for low-resolution powder patterns or triclinic or monoclinic symmetry materials remains difficult [43]. Indexing is the chief barrier in the powder XRD processes. Powder indexing performs best with high-quality data. Furthermore, with the expertise and experience of crystallographers and mineralogists, the growth in the number of various indexing algorithms used in the analysis of a powder sample enhances the possibility of efficient identification. Generally, machine learning is becoming more popular, and XRD processes are not exempted from these recent developments. It has already been demonstrated that an interpretable machine-learning technique may be used to determine crystal systems and space groupings using XRD spectra [43].

With the advent of machine learning, scientists have advocated for the elimination of the necessity of manual adjustments in the course of the early phases of crystal structure

research, and findings based on machine learning have been attained with a reliability of greater than 90%. Another option is to use a deep learning algorithm to characterize multiphase inorganic substances, which provides phase indexing and quantification characteristics. This entailed the creation of a convolutional neural network model trained with 1,785,405 synthetic XRD spectra created by combining 170 inorganic substances. These trained algorithms correctly and quickly recognized complicated phases of inorganic compositions, with results that were 100% precise for phase indexing and 86% effective for phase-fraction quantification. Furthermore, the capability of artificial intelligence of identifying and categorizing noisy complicated conformations in XRD patterns has been hypothesized and is being developed [43]. With these possibilities, the data emerging from the structures of the critical and strategic metals such as REEs with similar properties can easily be identified using the XRD technique.

For instance, in open-air settings, rare-earth ion-adsorption clays (400 ppm each of Dy, Ce, La, Nd, and Y) were produced from kaolinite at varying basic pH levels [44]. The effects of pH on the sorption process of REEs on kaolinite were studied using XRD, ICP-Ms, and X-ray photoelectron spectroscopy (XPS). According to XRD studies, the crystal structure of kaolinite does not change following REE sorption, indicating that REEs are attached to the exterior of kaolinite. Elemental characterization using ICP-MS and XPS revealed that the quantities of REEs on the surface of kaolinite are pH dependent, with a local optimum at pH 10 [44].

1.5. Recovery of the Metals

People had learned thousands of years ago how to construct furnaces and utilize fire to dissolve rocks and generate metals. However, the introduction of aqueous systems for mineral extraction came much later, primarily during the time of alchemists when alkalis and acids were discovered and used. Technologically advanced hydrometallurgy, on the other hand, can be linked to the late 1800s, when two main processes were invented: the cyanidation process for Au and Ag retrieval and the Bayer method for bauxite treatment [45]. Later, in the 1940s, a major development in U recovery occurred during the Manhattan Project in the U.S. From then, it advanced steadily, even substituting some pyrometallurgical systems.

The extraction of high amounts of metals from various sources is very vital for the mining industry and, by extension, for global economic growth. The most prominent metal recovery techniques in the mining industry are pyro-metallurgy, electrometallurgy, and hydrometallurgy. Pyro-metallurgy is metal recovery by the thermal treatment of an ore deposit, while electrometallurgy is metal recovery by the electrolysis of ore deposits. On the other hand, hydrometallurgy is the method that involves the recovery of metals through the leaching process in which the solid sample is mixed with a leaching agent with the capacity to dissolve the solid material [46]. Another important argument in favor of the development of hydrometallurgy is a significantly lower energy demand than in the currently used pyrometallurgical processes. Environmental considerations have become an important aspect in determining the direction of development of today's technology. Methods are sought whose impact on nature are as low as possible. The current environmental protection strategy assumes that today's technology should have the least possible impact on the natural environment and that all activities that will be carried out are to reduce pollution to the lowest possible level. In this light, hydrometallurgical methods gain additional importance in the extraction of metals from ores [21].

Conventional methods used in the metallurgical industry emit significant amounts of toxic or greenhouse gases such as SO_2, carbon dioxide, CO, and others into the atmosphere around the plant. SO_2 can be converted almost completely into H_2SO_4 acid if its concentration in the waste gas is sufficient. The problem arises when the SO_2 content is so low that the acid treatment method cannot be applied. Additionally, in metallurgical furnaces, dust containing Pb, Zn, Sn, Rh, Se, and other elements—together with the waste gases that pollute the environment—must be retained in the dedusting processes. This

leads to the need for additional devices [21]. In hydrometallurgical processes, we deal with methods that burden and pollute the natural environment to a much lesser extent, which is an important argument for the continuous development and modernization of this method of obtaining valuable metals.

Hydrometallurgy also can recover trace concentrations and this is a process that starts with leaching (Figure 2). After leaching, the separation and recovery steps are essential in reclaiming the desired metal(s) since the leaching step is neither perfect nor selective, allowing various contaminants to be available in the solution [47]. Some of the separation and recovery methods available include precipitation, solvent extraction, adsorption, and ion exchange [48,49]. Hydrometallurgical techniques use classical chemistry concepts such as variations in binding affinity, speciation, solubility, hydrodynamic size, and the redox characteristics of aqueous/organic partition to produce effective separation [19].
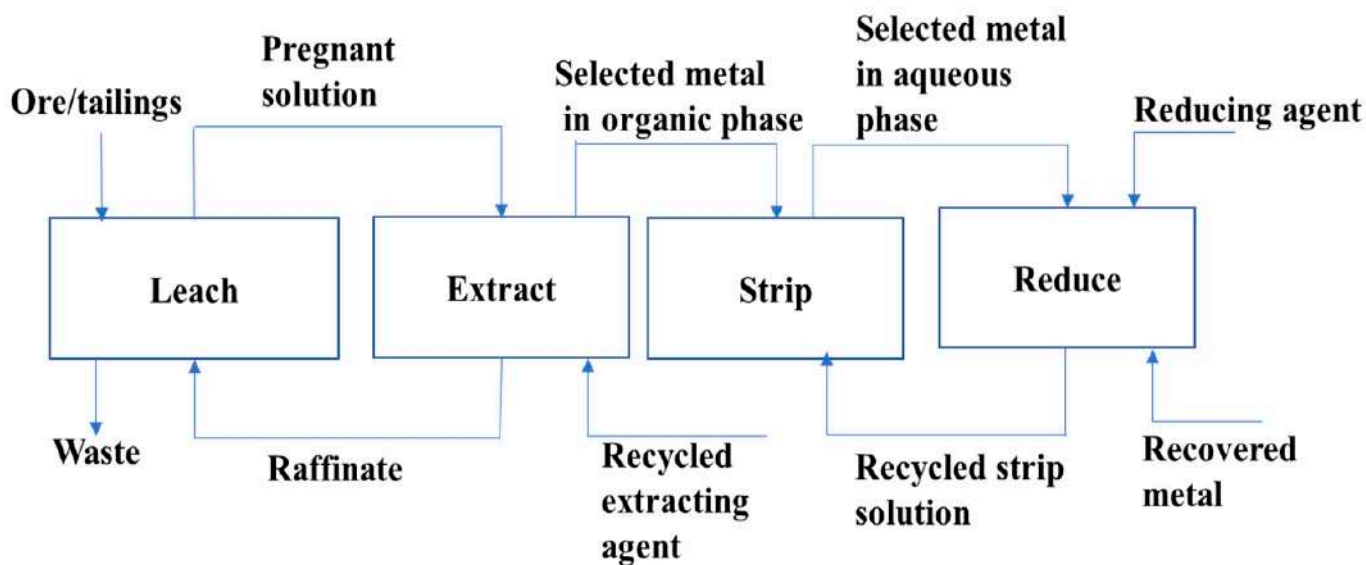

Figure 2. General scheme of hydrometallurgical processes.

The invention and use of hydrometallurgical advancements is a solution that is attainable for the high efficacy of recovering the metals. The main source of critical and strategic metals is ore. However, some metals can be recovered from various other sources such as waste from the mining industry, electronic waste, radioactive nuclear waste, seawater, and other sources. For instance, radioactive nuclear waste has been widely associated with lanthanides and actinides, which are critical for the modern economy. Nonetheless, due to the risks of radioactive REEs, it is essential to extract them from wastewater for radionuclide recovery [50]. There are also other wastes from the mining industry containing both valuable and harmful metals. Therefore, besides the economical point of view, the hydrometallurgical method can also help in reducing the harmful environmental effects of the waste discarded in a mine's neighborhood or other wastes discarded from related industries [51]. Metal recoveries have drawn the interest of numerous researchers for quite some time now, and the need for creating new techniques of remediation has emerged as the need of the hour. Traditional methods have been in use for decades and have produced excellent results, but they have their drawbacks [52]. The creation and optimization of the hydrometallurgical processes using modern nuclear techniques might be the future of the mining industry.

2. Role of Nuclear Technologies and Nuclear Analytical Methods in the Advancement of Hydrometallurgical Processes

The period of the most prolific development of basic research in radiochemistry and nuclear chemistry was the first four to five decades of the past century. If we consider

the birth time of these scientific disciplines to be 1898, the year of the discovery of Po and Ra, a proper understanding of the surprising results of physical experiments revealed a new field of radioactive chemistry to researchers. Thanks to this, it was possible to obtain and test completely new substances and study the new properties of known substances in the previously unavailable field of trace analysis. These properties are often different from those observed in the area of classical macro-quantity chemical analysis. The end of this period of great discoveries was marked by the discovery of nuclear energy and the formulation of the basic laws of nuclear physics, which marked a breakthrough in the world of 20th century science [53].

The majority of the separation procedures were developed in the frame of radiochemistry and nuclear chemical engineering. In the early years of radiochemistry's establishment as a field of science, ion exchange, extraction, precipitation, and other separation methods were studied and implemented. Complete sets of analytical control methods for nuclear chemical technology have been developed. The numerous nuclear techniques used in analytical chemistry have significantly extended the possibilities of classical analytical methods. The development of Neutron Activation Analysis (NAA), which, in combination with radiochemical methods of separating metal ions, belongs to the group of inorganic trace analysis methods known to have the best low detection and quantification limits [54]. Energy Dispersive X-Ray Fluorescence (EDXRF), Total Reflection X-Ray Fluorescence (TXRF), and XRD are other important analytical techniques that play principal roles in the characterization and quantification of the various elements in the periodic table [55–57]. Most importantly, the use of radioactive tracers is also an extremely valuable tool in the creation of new purification/separation methods for the needs of NAA and radiochemical research, but these are also used in conjunction with other techniques of instrumental analysis. The radioactive isotopes of many elements are also used in numerous variants of the isotope dilution method. Isotope markers for the study of hydrometallurgical processes are very broad. They are useful in studying processes such as flotation [58], leaching, sorption, extraction, precipitation and co-precipitation, and electrolysis in aqueous solutions. Radiotracer methods are used in both laboratory and industrial research. Hydrometallurgical processes aim to obtain metals or their compounds from ores, concentrates, tailings, and wastes [59].

Mining, exploration, metallurgical, and mineral industries are irreplaceable in the progress of the current society. As the global consumption of metals rises and larger low-grade deposits are extracted to meet demand, economic and sustainable mineral processing will demand technological innovation. The creation and implementation of unique instruments to offer the real-time control of mining and mineral processing plants for enhanced control have the prospective to support the metal recovery improvements of a broad range of commodities [60]. Nucleonic control and analysis systems, radiotracer technologies, and other relevant nuclear advancements are suitable for optimizing metallurgical industries with relevance in realizing the technical and economic benefits in the future [61].

In the study of hydrometallurgical issues, the following methods of nuclear technology are primarily useful:

— the method of isotope tracers for studying the physicochemical foundations of processes; laboratory industrial technology studies, a method for researching the effectiveness of existing industrial technologies and apparatus; and the control and regulation of industrial processes;
— radiometric analysis, such as the neutron activation method, X-Ray Fluorescence spectrometry, and others, due to the possibility of rapid analysis without destroying the tested material and the possibility of operating with very low concentrations;
— the use of nuclear equipment to control and regulate technological processes.

The major fields applying nuclear techniques encompass the exploration of delineating the ore deposit, deposit value evaluation, and elemental analysis. In mining, nuclear techniques assist in evaluating subsidence in mines, monitoring gas leakage, tracking the in situ leaching process, and assessing the slope stability and caving process [62,63]. However, in

mineral beneficiation processing, nuclear techniques are useful in mass balancing, efficiency evaluation of the unit operation, grade determination, ore sorting, and monitoring process dynamics [64]. Many pyrometallurgical processes were optimized in their development stages due to the possibility of using the radiotracer technique [65–67]. In chemical extraction encompassing pyro-metallurgy, electrometallurgy, and hydrometallurgy, nuclear methods are applicable in monitoring high-pressure and temperature processes, efficiency evaluation of the unit operation, and tracking highly corrosive processes. Nuclear techniques are also vital in leakage detection and evaluation, the management of mining waste, energy, and water monitoring of the transport of pollutants via ground and underground water plus soil [62]. However, the most important part of the mineral industry is the recovery processes, with hydrometallurgy emerging as the best approach due to its ability to reclaim trace amounts of minerals. In our view, the application of nuclear techniques in metal separation can be summarized in Figure 3.
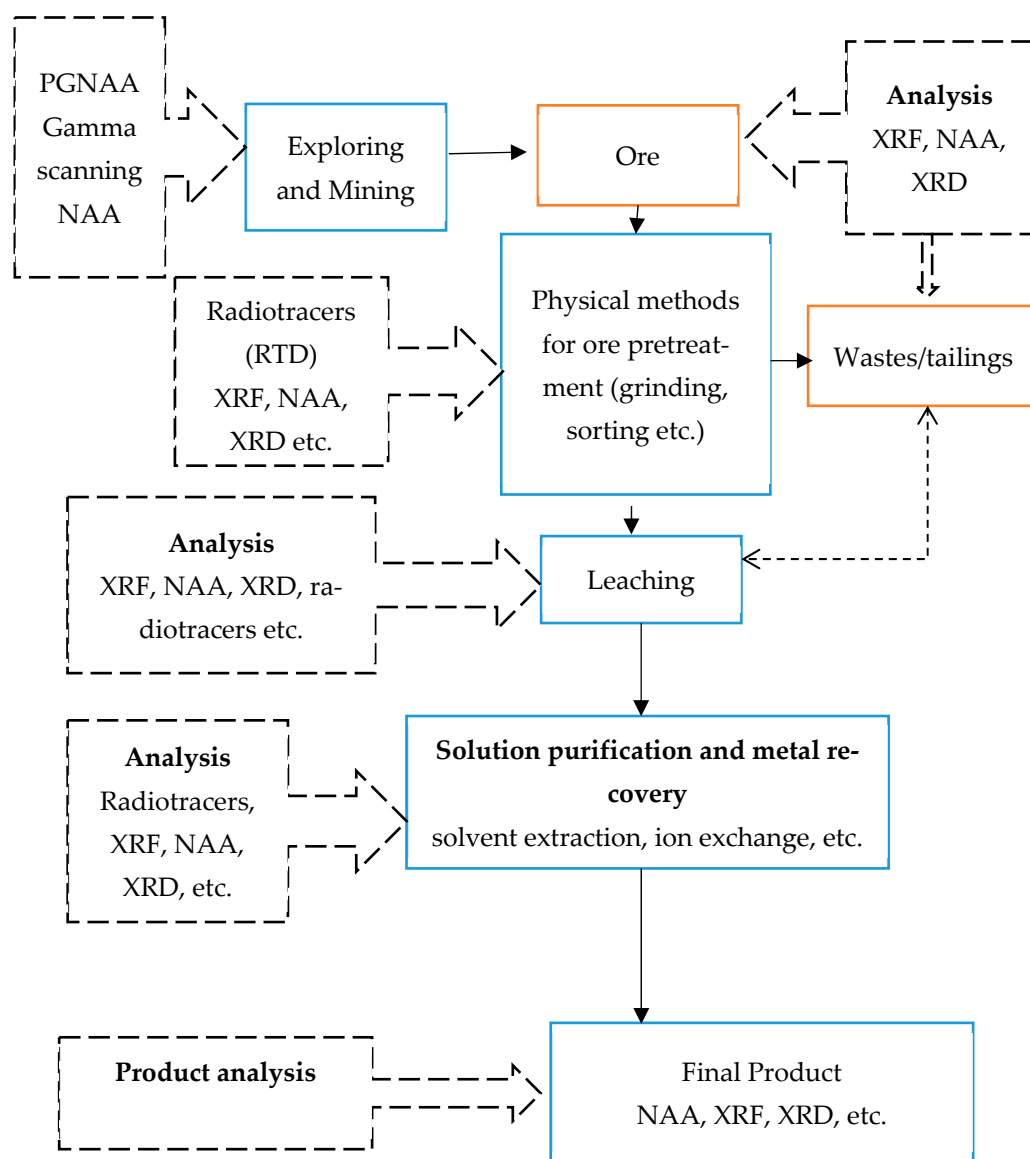

Figure 3. Nuclear techniques for hydrometallurgical processes.

2.1. Development of Nuclear Techniques for the Study of Metals and Recovery Using Hydrometallurgical Processes

2.1.1. Neutron Activation Analysis (NAA) of the metals

All mineral exploration is principled on a broad knowledge of natural formations and the geochemistry of the area being studied. Nuclear methods are specifically beneficial for learning about the distribution of metals in various sample types. NAA has been extensively applied in basic geological studies to analyze elements [68]. NAA is a sensitive analytical method crucial in conducting both the identification and quantification of the minor, major, and trace metals in the samples from nearly every imaginable field of technical or scientific interest [69]. In NAA, the nuclear reactions take place through the bombardment of the sample to be examined with neutrons. The reaction products to be examined are either the released radiation immediately upon neutron capture or the resultant new nuclei are radioactive due to the induced radioactivity that will make them decay in due course.

The induced radioactivity on the substrates is the most prominent mode of NAA. All the stable metals have suitable properties for the generation of radioactive isotopes, although at distinct reaction rates. The elemental selectivity of Instrumental-NAA (INAA) is always excellent because the purity and identity of the radionuclide analyzed may be confirmed by the half-life and its radiation energy. Additionally, the technique is suitable for metals with high-neutron-capture cross-sections where the maximum sensitivity is realized. Apart from the elements of interest, INAA can give the concentrations levels of other elements in the sample [70].

For many elements, NAA represents a non-destructive and accurate analytical technique that is simple to automate and use to conduct multi-element analysis. Over 40 distinct elements in rock/ore samples can be ascertained using I NAA. When analyzing Sb, REEs, Au, PGMs, U, and Th in ordinary rock samples, NAA outperforms non-nuclear techniques [68]. NAA is an attractive method in the analysis of REEs and heavy metals in samples, such as sediments, air particulate, soil, and water, among other materials [71]. Qualitative analysis is important because it assists in the identification of the metals present in the sample for the appropriate development of their recovery process. Phosphate ore samples from Egypt were analyzed during the determination of ^{232}Th, ^{238}U, REEs, and other elements present [71]. The study showed that INAA can analyze the different amounts of elements in the phosphate ore (Th, U, Cr, Eu, Ce, Co, Hf, La, Sc, Rb, Lu, Nb, Sm, Sn, Zr, and Yb, among others). Trace elemental measurements of rock samples are critically valuable because these rocks can be used as a coarse aggregate in concrete types that may be established for shielding accelerator and reactor facilities [72]. Geoscientists can comprehend the chemistry of rock formation by analyzing REEs and other trace elements in geological samples.

The INAA technique can also be used to track the chemical processes occurring during the recovery of the metals. That possibility enabled the use of INAA in the hydrometallurgical extraction of $PbCl_2$ from the ore concentrate of the zone of Herzegovina Vares, Bosnia [73]. The technique assisted in the radiochemical determination of the elements and tracking the dissolution of PbS from concentrate. That was possible because the activation analyses, such as isotope dilution NAA, are free of interference, making them suitable for the analysis of metals such as Hf which is an impurity of Zr compounds existing at 2% to 3%. Zr and Hf are very critical in the nuclear industry, where they are sourced from the Zr ores, whose recovery process demands Hf of less than 100 ppm. For that reason, during the hydrometallurgy, the combination of ICP-MS and NAA helps evaluate the quantities of Hf in $ZrSO_4$ solutions with lower scattering [74].

In a similar study, INAA was used in the analysis of the Au in the Au ores from Egypt [70]. The INAA technique was used even though there were recently developed non-destructive methods such as Fast-NAA (FNAA) available that are fast, accurate, and require only small quantities of samples for analysis. However, FNAA is applicable when the material comprises large quantities of Au and when the counting time is long. INAA, on the other hand, is based on the determination of the elemental weight in the sample

through the measurement of the induced radioactivity. From the gold ore analysis, ^{198}Au with a half-life ($T_{1/2}$) of 2.7 days and characteristic energy of 411.8 KeV was activated. The ^{198}Au was found to be 25.7% in the sample. Other metals, such as ^{51}Ti with $T_{1/2}$ of 5.8 min at 320.1 KeV, were activated, and the amount was reported to be 0.46% in the Au ore [70]. That means the method can not only be used in measuring the elements of interest, but can also give information about the rest of the activated metals present in the sample. In some cases, the INAA can be coupled and used together with the Prompt Gamma Analysis (PGA) method. PGA is a non-destructive analytical technique in which a neutron beam is used to excite materials, causing elemental nuclei to collect neutrons and release specific rapid gamma rays during de-excitation. The technique is only applicable for elemental analysis during the sample's irradiation in the research reactor or neutron generators. The PGA and INAA were applied while conducting a study on the mine tailings from small-scale gold mining in Paracale, Philippines [75]. PGA and INAA were used to evaluate the elemental contents of Au and Hg in tailings. The two techniques were used because PGA activates the samples with neutrons which can be measured by INAA after two days. For that reason, the samples do not require neutron activation in the nuclear reactor.

2.1.2. XRF Spectrometry

XRF Spectrometry is an analytical method that employs X-rays to excite atoms in a specimen. When a sample interacts with high-energy X-ray beams, its atoms are energized in the inner shell, causing them to be accelerated to higher energy levels, which leaves a hole (positive) where the electron was. The excited atom is unstable in the outer shell, and as a result, it de-excites to the ground state with the discharge of the characteristic energy of the particular components present [55]. The intensity of the signal produced due to the incoming photon is then measured by a silicon drift detector with high counts and good resolution. The amplitude of the pulse is proportional to the energy of the acquired characteristic X-rays [76]. The multichannel analyzer stores such data based on its amplitude, which is then formatted to an X-Ray Fluorescence spectral line for qualitative and quantitative analysis.

EDXRF is majorly applied in the evaluation of the elemental or chemical conformation of a material [77]. The technique uses X-rays to excite atoms in the material, which release X-rays as they de-excite at energies specific to each metal. The characterization abilities of this technique depend on the exclusive atomic structure of every element, which permits a unique set of signals in form of peaks to be identified from the electromagnetic spectrum [78]. A chemical mapping study on the mine waste drill cores was conducted using the EXDRF and Laser-Induced Breakdown Spectroscopy (LIBS) spectrometers during the mineral exploration [79]. The basis of the study was the remediation of the metals from the waste from mining activities in the east of Aachen (Germany). The approach was employed because the EDXRF spectrometer is capable of detecting the majority of elements ranging from Al to U [79]. The elemental concentrations obtained provided the basis for mapping the elements in the mine wastes from the Pb–Zn drill cores, which enabled the researchers to correct the matrix from the scanners and predict the quantities of the elements in the wastes using a model. However, both techniques suffer from the matrix effects that need to be corrected for both quantitative and semi-quantitative analysis of mining wastes.

A related study was conducted in which the scholars applied the EDXRF method in the elemental analysis of the mine wastes [80]. The components (Ti, Rb, Sr Cr, K, Ca, Ni, Cu Mn, Fe, Co, Zn, and Pb) were identified and quantified utilizing the fundamental principles technique. The Cu, Zn, Cr, Ni, and Pb contents were compared to the concentrations from E.U. and Spanish regulations. The idea was to assess the ecological hazard and designate the pollutants as inert wastes or dumps that must be controlled and land-filled. Apart from the concentration levels of Zn and Pb, the results showed that the wastes were inert for the metals under consideration. The study concluded that EDXRF is a fast and valid investigative method for examining the mine tailings' elemental composition. The findings from the EDXRF can assist in the classification of the method to be applied in the disposal

of mining wastes [80]. The method can also be applied in determining the geochemistry of the sedimentary mining cores in polluted regions, since the technique guarantees high resolution [81]. That is because the method has significant capabilities of analyzing the material directly after piercing the core in half.

There are numerous applications of nuclear techniques in ore processing, metal remediation, and purification. In varying phases of the processes, nucleonic control systems, tracer methods, and elemental analyzers can be used. The most popularly utilized nuclear method in ore processing is XRF spectrometry, which allows the real-time analysis of metals. Few firms around the globe sell commercial XRF analyzers, and many installations are in operation [68]. The technique offers the opportunity to analyze multiple processing points at the same time. Typically, the input material, tailing, and final product can be examined using the XRF. Two distinct systems are commonly put into consideration where the probes are implanted into the pipes or containers of the primary process in one version. One automatic sampling in the other one is carried out and the samples are transported to the analyzer via pipes. With a single probe, multiple elements can be resolved at the same time.

The technique, when coupled with synchrotron light sources, can play a great role in the acquisition of reliable levels of spatial resolution in core scanning assessment. The main advantages of XRF techniques include their simplicity, fast operation, non-destructive nature, and minimum sample preparation. However, the chemical contents of the matrix harshly impact the intensity of the obtained analyte line during the sample analysis [82]. Therefore, matrix-matched standards are necessary for a precise and accurate evaluation of the elemental composition of the sample. The elemental composition from XRF- and INAA-based techniques is very important in the recovery process because it helps in the selection of the remediation methods based on the elemental quantities in the sample.

2.1.3. XRD

Mineralogy is an important parameter in the characterization of sedimentary formations and affects the design process in commercial operations [83]. XRD is a robust analytical method that is very useful in the characterization of various samples. It is an established approach used on samples from igneous, sedimentary, and metamorphic formations where characterization is based on the databases containing thousands of mineral spectra. However, there are difficulties in using XRD for the quantification of minerals, such as preferred-orientation impacts. Mineral valuation by XRD tends to be especially reliant on the operators' sample preparation and interpretation methods, rather than XRD analytical capacity [83]. Because X-rays have wavelengths atomic in size, XRD-based techniques are applied in the extraction of useful information about atomic structures [43]. The technique is non-destructive, and it can evaluate a broad range of materials, such as polymers, minerals, metals, plastics, semiconductors, solar cells, and ceramics.

The XRD method relies on the dispersing of X-rays by electrons in the respective components of a crystal. Once X-ray radiation impedes the surface of a crystal substance at an incidence angle, a portion of the beam is diffracted by the atoms on the surface, and the proportion that is not dispersed hits atoms deep in the crystal lattice, in which a portion is dispersed [84]. These scattered waves, which are released in various directions, interfere with one another. Interference can either be destructive or constructive (diffraction), and this is reliant on the kind of wave interaction and its direction. The regular configuration of atomic structures in solids generates constructive interference [43,84]. As a result, the scattered beam is formed only if the specific geometrical criterion is met, as defined by the Bragg equation [84]:

$$N\lambda = 2d\sin\theta \tag{1}$$

wherein λ is the X-ray beam's wavelength, d is the interplanar spacing of the crystal, n is an integer representative of the magnitude of reflection, and θ is the X-ray beam's angle of incidence or reflection. The optimal crystal size for Bragg reflection is typically between 10^5 and 10^7 m, and if the size of the crystal is less than around 10^8 m, it will be very minute for diffraction at Bragg angles, limiting its constructive interactions to low angles.

It is simple to explain the XRD spectra of crystalline material compared to amorphous substances [43]. These possibilities are important in the hydrometallurgical recovery of metals. Numerous analytical techniques have been used to examine the behavior and conversion processes of a broad range of hydrometallurgical aqueous solid phases. Apart from XRD, X-ray photoelectron spectroscopy (XPS), and X-ray absorption spectroscopy (XAS) can also be used in the analysis of solid phases. XPS has become one of the most widely used surface analysis techniques, and XPS instrumentation has become more user-friendly, making the technology available to a large number of researchers [85]. XPS can detect the elements present in a solid surface up to a depth of 10 nm, and can provide insights into unstructured minerals with much smaller crystal sizes [84].

On the other hand, transitions are involved in the absorption XAS, or emission (X-ray emission spectroscopy) of X-rays, in which the former evaluates the movement of the element from the ground level to the excited level, and the latter examines the decay processes from the excited state to the ground state. All these techniques classify the chemical conditions and nature of atoms in molecules. The assessment of the transformation from elemental primary electronic states to high electronic states and the continuum is recognized as X-ray Absorption Near-Edge Structure (XANES), and the latter is for analyzing the fine structures and is classified as an Extended X-ray Absorption Fine Structure (EXAFS), which known to work well for absorption processes at energies above the minimum level for electron emission. The XANES spectra describe the electronic configuration and orientation of the metal location, whereas the EXAFS provide types, numerical data, and ranges to ligands and adjacent atoms from the absorbent metal [86]. A combination of surface analysis and structural techniques offers a great opportunity of understanding the configuration of the elements in the sample under assessment.

Ex situ approaches have produced major breakthroughs in understanding the characteristics of the final phases and the processes by which they alter reaction speeds. This implies that the stages included in solid-phase transitions were not followed in situ. Moreover, because the samples under study were excluded from the reaction setting, the solid interfaces might have been changed before the characterization studies [84]. Since crystalline phases are common in aqueous environments, on-site XRD has given substantial data on reaction pathways and kinetics, crystal size, and the type of crystalline and amorphous transitional product stages against time. Even though a normal workroom diffractometer with a Cu Kα X-ray source can sometimes be utilized to carry out in situ analysis, the nature of the obtained signal is prone to errors due to aqueous-phase retardation inside the reaction cells. Through the application of concentrated and intensive high-energy X-rays able to traverse a broad variety of in situ sample conditions, the synchrotron beam allows XRD studies to be conducted with great spatial and temporal precision [84].

Synchrotron radiation fills a unique niche by allowing XRD analysis with higher energy, spatial, and temporal precision. Synchrotron sources generally offer an array of X-ray energies appropriate to the majority of metals in the periodic table [86]. On comparable-sized samples, a synchrotron beam is 10^4 to 10^{12} orders of magnitude brighter, and 10^6 times quicker at counting statistics than ordinary X-ray tubes. Due to the tremendous strength of synchrotron X-ray radiation, the signal-to-noise ratio is substantially improved, which allows the examination of minute quantities of samples. Other benefits of employing synchrotron X-ray radiations include the capacity to obtain high-quality data for Rietveld refinements and to modify the wavelength of the impinging radiation. Because of the wavelength's tunability, it is feasible to exclude absorption edges or employ harsh X-ray beams to enter reaction cells [84].

In situ S-XRD assessments can be performed using either energy or angular dispersive diffraction methods. A monochromatic X-ray source is used in angular dispersive diffraction (ADD), and the diffracted X-ray radiation is measured as a parameter of the diffracting angle, utilizing a two-dimensional position-sensitive detector or a one-dimensional position-sensitive monitor. Polychromatic radiation is utilized in energy dispersive diffraction (EDD) [84]. A solid-state monitor at a given angle, or many static angles, is used

to measure the energy distributions of the diffracted radiation. One benefit of utilizing consistent wavelength radiation for in situ S-XRD experiments is that the data acquired have a better d-spacing resolution, which permits structural measurements of the patterns resulting from the diffraction process. This approach has been applied widely in the analysis of sulfide-based minerals, among others.

The dynamics of sulfide mineral dissolution in chloride solutions have recently gained a lot of interest. There are various reasons for this attention, one of which is the advent of building materials with better resistance against chloride attacks. The most relevant aspect, nevertheless, is the significantly quicker dissolving rate of sulfides in chloride solutions [87]. In situ S-XRD methods are highly diverse explorative tools for increasing the interpretation of commercially significant mineral dissolution reactions. S-XRD was used to analyze the solid phase transitions in aqueous conditions, with a focus on hydrometallurgical processes such as the solubilization of lateritic nickel ores and sulfides such as bornite (Cu_5FeS_4), chalcocite (Cu_2S), and pyrite (FeS_2) [84]. At 25 °C, no alteration of the crystal lattice was detected, which is consistent with the mineral's well-known slow solubility rate. The development of covellite (CuS), metal sulphates (ferrous or cupric sulphates), elemental sulfur (S8), and chalcopyrite ($CuFeS_2$) atoms were seen at temperatures ranging from 100 to 200 °C (NFM). The findings showed that mineral transition to such product phases began around 10 min after the tests started and that the synthesis of elemental S may be attributed to the Fe^{3+} ion's preliminary oxidation of $CuFeS_2$, succeeded by CuS oxidation by the identical oxidants. The current findings, when combined with prior research, show that S-XRD approaches may be utilized to increase our understanding of essential hydrometallurgical processes [84].

Under heap bioleaching conditions, the most readily available Cu mineral, $CuFeS_2$, does not dissolve substantially. Mineral leaching rates are recognized to be particularly slow at minimum temperatures and generally decrease over time. A number of studies have been conducted in an attempt to circumvent this limitation, with the goal of understanding the kinetic parameters and factors behind the dissolution of this $CuFeS_2$ [88]. The $CuFeS_2$'s slow leaching kinetics has been attributed to the creation of an unsolvable layer, which inhibits the extra dissolution of the mineral. Even so, the nature of the product layer and the processes through which it forms and influences the dissolution reaction are not well understood. Under atmospheric conditions, characterization methods such as XPS, XRD, Raman spectroscopy (RS), and XAS, along with scanning electron microscopy (SEM) combined with electron probe micro-analyses (EPMA) or energy dispersive spectrometry (EDXRF), have been applied to enhance our understanding of the nature of the layers of the product formed on $CuFeS_2$ in the course of its digestion in acidic solutions [88].

One of the most productive and recyclable catalysts of $CuFeS_2$ bioleaching is Ag^+. Due to the difficulty of the surface reaction throughout $CuFeS_2$ bioleaching, there remains debate about the catalytic process of Ag^+ in boosting $CuFeS_2$ solubilization. A study explored the significant impact of Ag^+ on the bioleaching of $CuFeS_2$ through the thermophile *Acidianus manzaensis*. The pertinent Fe and S speciation of leaching by-products was evaluated using XANES and S-XRD spectroscopy [89]. Bioleaching tests demonstrated that incorporating Ag^+ substantially increased Cu extraction, with 0.05% being the optimum amount of Ag^+ (mass fraction of Ag^+ to $CuFeS_2$). The transitional S_0, jarosite, and secondary mineral deposits (chalcocite, bornite, and covellite) were established throughout bioleaching under the conditions of the availability of 0.05% Ag^+ and the apparent lack of Ag^+, according to S-XRD and XANES assessments. The inclusion of Ag^+ boosted the generation of covellite and bornite while having no influence on the production of chalcocite, denoting that the bioleaching of $CuFeS_2$ must be catalyzed by Ag^+ to enhance the production of bornite and its transformation to covellite. The quick production of bornite-like species aided the beneficial impact of Ag^+ on $CuFeS_2$ bioleaching, whereas the buildup of covellite decelerated the leaching degree at the final moment of the $CuFeS_2$ bioleaching time frame [89].

XRD was also employed in a pyro-hydrometallurgical process that included leaching, roasting, and precipitation steps to extract Pb, Sb, and Sn from lead dross (LD). Sb and

Sn have been identified as critical metals that will support the technologically advancing economy [90]. The industrial consumption for these metals is increasing, while their sources are decreasing. As part of their separation processes, the calcine from the two-stage roasting was desulphurized with a 2 M Na_2CO_3 liquid for leaching using HNO_3. The formation of Na_2SO_4 during the process was an essential factor evaluated in this stage to maximize Pb recovery [91]. Before the HNO_3 leaching, the deposit from desulphurization was filtered and washed. Based on the ICP–Optical Emission Spectrometry (ICP-OES) measurement of an aqueous sample after leaching, over 99% of Pb was leached at temperatures over 50 °C [91]. For the retrieval of Sn and Sb, a remnant from Pb leaching was taken for the next steps. At this point, unsolvable Sn and Sb oxide were retained in the residue, and XRD analysis revealed that Sn and Sb oxide were important components. In addition, the leached mixture was neutralized to precipitate $PbCO_3$ through the application of a 2 M Na_2CO_3 medium to adjust the pH. The Pb precipitation test was timed, and more than 99% of the Pb was recovered through precipitation within the first 5 min. The precipitate's XRD examination findings revealed that $2PbCO_3Pb(OH)_2$ and $PbCO_3$ were key components in the Pb end product. Sb was extracted as Sb_2O_3 from Sn (SnO_2) at a pH of less than 8, and the elements of the recovery processes were verified using XRD [91]. XRD separation is critical in validating the structure of the accessible components in the final residue.

The relevance of transition metals and REEs in various industries is well recognized, and their significance in high technology is growing. A study was carried out to evaluate the dissolution kinetics of Nd (35 wt%) in magnetic effluents under HNO_3 or HCl acid media, with the extraction of Fe as $Fe(OH)_3$ preceded by precipitation using oxalic acid to retrieve Dy and Nd. The XRD technique was then applied in the analysis of the samples during which all solid specimens were examined in a constant scan mode at a scan rate of 5°/min between 10° and 80° 2θ [92]. The XRD assessment of neodymium oxalate hydrate [$Nd_2(C_2O_4)_3 \cdot 10HO_2$] precipitate was achieved by the slow and rapid addition of oxalic acid. Slow oxalic acid incorporation promoted the formation of the precipitate and crystallization, unlike the rapid addition. That was supported by the variations in peak intensities of $Nd_2(C_2O_4)_3 \cdot 10HO_2$ from the XRD analysis. The precipitation using oxalic acid resulted in the recovery of 91 to 92% of the Nd in the mixture and overall precipitation of 70 to 72% at this level, compared to the original amount of Nd [92]. Likewise, the remediation of Dy was found to be 65 to 78%, for a total retrieval of 53 to 60%. Additionally, the XRD and chemical analysis confirmed that Fe was removed completely in the course of precipitating Fe.

Numerous hydrolysis–precipitation techniques for Fe recovery from hydrometallurgical solutions have already been established since the early 1970s. The jarosite process, hematite process, and goethite process are a few instances of broadly applied techniques. The goethite process has lower CAPEX than the hematite process and produces more environmentally safe yields than the jarosite method [93]. The vital component of the goethite process is that the Fe content should be kept below 1 g/L throughout the precipitation process. This demand is fulfilled by either the reduction of all Fe^{3+} to Fe^{2+}, which is a process identified as the V.M. method. For the goethite approach, however, the precipitates are "amorphous Fe phases," which are most probably the nanoscale minerals schwertmannite or ferrihydrite. A study that used the V.M method to carry out the goethite procedures at a reduced pH level discovered that the Fe could partly precipitate as magnetite. By magnetic separation or magnetic flocculation, the magnetite particles compensate for the precipitates' poor settling and filterability abilities. XRD and scanning electron microscopy (ESEM) assessment provided a deep understanding of the precipitate features. Controlling the pH and oxidation potential value allowed the Fe ion to partially precipitate as magnetite. Magnetite particles aid in the effective removal of liquids and solids via magnetic flocculation and separation. Magnetite precipitation offers a new approach to removing Fe from the nickel-rich mixture, but it must be enhanced through extensive experimental studies [93]. It is indisputable that XRD and the related nuclear techniques play a very

significant role during the recovery of the metal by offering a reliable phase characterization of the elements of interest.

3. The Radiotracer Methods

Radiotracer methods are among the nuclear techniques applied in the mining industry and remediation of different metals from broad sources, from the perspective of economic and environmental protection. A radioactive label, or radiotracer, is a chemical composite in which one or more atoms have been substituted by a radionuclide [94]. Numerous radiotracers are available based on their activation energy, cost, half-life, availability, and chemical or physical properties. The radiotracers are usually utilized for several applications in manufacturing systems due to their advantages such as in situ detection, high detection sensitivity, limited memory effect, and physicochemical compatibility [95]. These make radiotracers reliable due to their rapid response leading to accurate results [96]. The radiotracer also vanishes from the tagged sample with time; therefore, any impurity caused by radiation is detached automatically because of the radioactive decay characteristic of the radiotracer [97]. Radiotracers can also be used in harsh environmental conditions to check the performance of the process. Only a small quantity of radiotracers is required for monitoring a process because of their high detection sensitivity, and they do not alter the flow dynamics inside the system. Additionally, the real-time control of the presence of an extensive range of well-matched radiotracers makes them ideal for tracing the processes of the samples in manufacturing plants [95].

Radiotracer technologies have helped technologists and engineers to diagnose faults and process anomalies and mechanical damage without plant disruption or the need to shut down the working processes. The technology has garnered general acceptance globally. The deployment of radioisotope-based technology is a quickly developing a function in supporting the industry in improving its manufacturing efficiency and optimizing plant operation [96]. Detectors such as scintillation radiation detectors are majorly used in radiotracer analysis because they can detect gamma rays transmitted by the radioisotope through the walls of the system. High-Purity Germanium (HPGe) radiation detectors are also useful when performing laboratory-based analysis. The signals detected by such probes are recorded in a data acquisition system integrated into a computer system [98]. For that reason, selecting an appropriate radiotracer is very critical for a specific research/study [39]. The half-life, physicochemical behavior, type and energy of radiation, specific activity, and radiotoxicity are the central properties acknowledged in the selection of a radiotracer.

The radiotracer technology's distinguishing feature is its capacity to deliver information that cannot be accessed through other methods. This technology has been extensively employed to help unravel industrial hitches in advanced economies, but it is still underutilized in Global South nations due to the lack of radiotracers at the point of need. It is required to import radiotracers for Global South countries that do not have radioisotope manufacturing facilities, and the long amount of time needed in this process eliminates the prospect of realizing the prospective benefits of this technology [99]. The gap can be partially addressed by building or installing affordable neutron generators or sources and research reactors in these countries through local and international support. That will allow scholars from the Global South countries to develop various techniques and approaches based on radiotracers, such as the optimization of metal recovery using radiotracers.

3.1. Application of Radiotracer Techniques in the Optimization of the Chemical Processes in Hydrometallurgy Using RTD

For a wide range of reasons, radiotracer techniques are commonly employed for mineral processing examination and optimization. The majority of operations in mineral processing are carried out on a massive scale. As a result, the level of effectiveness is not always as it is projected by the pilot scale tests. Advancements in industrial processes lead to significant savings, and radiotracer methodologies provide unique opportunities to study their behavior. Radiotracer methods are used to study blending, material flow,

and crushing, among other things [68]. Other applications entail the investigation of physicochemical reactions, the separation of slag and metal, the evaluation of process material volumes in tanks, and the wear of tanks. Radiotracer methods are also employed in quality control to detect non-metallic inclusions in metals.

In the application of radiotracer techniques in flow analysis, Residence Time Distribution (RTD) is an essential parameter [100]. RTD is a probability distribution model that predicts how long a fluid element stays in a reactor. It aids in reactor troubleshooting and describes the flow and mixing within reactors [101,102]. RTD is vital in evaluating the design of the continuous operating chemical process system and optimizing its working parameters. Radiotracer techniques are utilized in the measurement of the RTD of process material in full-scale and pilot industrial systems [103]. The approach assists in the determination of flow parameters such as bypassing, Mean Residence Time (MRT), degree of mixing, and extent of the dead volume. The concept of radiotracers in troubleshooting investigation and process optimization in numerous industries has attracted technologists and scientists because they allow small quantities of a radioisotope to be precisely evaluated [98]. They offer many benefits, including the best detection sensitivity and the ability to offer real-time measurements [101,102]. The RTD is a frequently used concept for characterizing flow in chemical reactors and determining the MRT of process fluid [104]. Radiotracer technology is a cutting-edge technique for optimizing industrial processes and troubleshooting because of its great sensitivity, improved statistics, online measurement, and high benefit-to-cost ratio [99,101].

In the chemical, hydrometallurgical and associated industries, mechanical mixing is one of the most prevalent procedures. The classical impulse-response methodology has been widely utilized to investigate and analyze the nature of homogenization using colorimetry, pH metric, thermometry, and conductivity methods [105]. These approaches necessitate the placing of the probe inside the reactor, which causes liquid mobility to be interrupted. The radiotracer approach enables the continuous monitoring of the mixing process by analyzing the tracer concentration through the device's wall. Furthermore, only this technology can be used on large-scale industrial equipment. A scintillation detector was positioned outside the tank near the injection point to observe the mixing processes as a small volume of the ^{99m}Tc radiotracer was quickly and lightly introduced under the liquid surface [105]. The volume "seen" by the probe was controlled by encasing it in a 2 cm diameter hole in a ring of lead. The behavior of the fluid in the reactor fits the tanks-in-series with recycle model, according to the analysis of the experimental and simulated curves for each rotational speed. That means it could be utilized in the characterization of fluid mixing [105].

3.2. Application of the Radiotracer Techniques in Leaching

Leaching, which entails the use of solutions to digest a sample, is a key component of hydrometallurgy. Hydrometallurgy preferentially dissolves and precipitates metals using strong organic acids/inorganic or caustic liquid solutions. Acid leaching is a classical hydrometallurgical separation process used to retrieve metals. HCl, HNO$_3$, H$_2$SO$_4$, HClO$_4$, and aqua regia are often used in the leaching of various metals from diverse materials [106]. Substantial quantities of chemicals are employed in hydrometallurgical methods, and the overall processes are lengthy and highly complex. This necessitates the optimization of the metal leaching process in various mining industries, such as Cu recovery.

For instance, the primary technology used in the Polish Cu industry is the pyrometallurgy technique in shaft blast furnaces and one-stage flash furnaces, which is continuously being enhanced. Substantial amounts of Cu, Ag, and other metals are still present in post-production tailings and wastes. As a result of the substantial costs of producing Cu and the potential of recovering other metals, a hydrometallurgical process could be used to find a solution. A study was conducted with the scientific goal of developing and optimizing the primary step of the hydrometallurgical Cu recovery processes (leaching and solvent extraction) using radiotracers [51]. The utilization of the radiotracer in the research was

meant to replace the conventional steps in the quantitative analysis of the metals during which a real-time evaluation of the metallic concentrations was viable during the leaching process [51]. The ^{64}Cu isotope was chosen as the radiotracer during the optimization of the leaching process of Cu from the floatation tailings. A two-step leaching system was studied and the research showed that approximately 80% of Cu can be recovered using an HNO$_3$ concentration of 5 M (Figure 4).
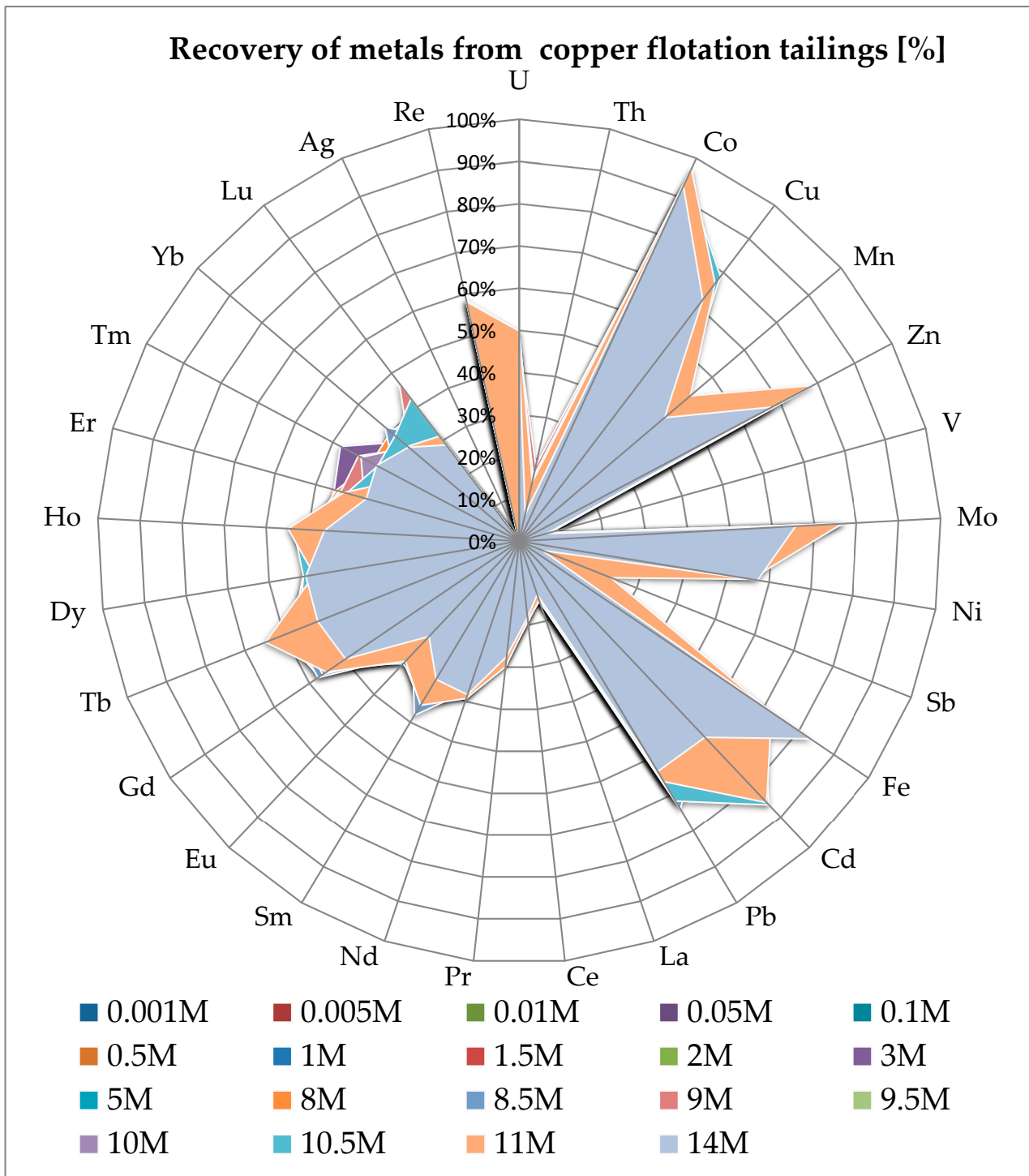

Figure 4. Metals recovery efficiency results from flotation tailings with HNO$_3$ using NAA as an analytical method.

The leaching time was evaluated using the radiometric method. The irradiated sample was placed into a stirrer chemical reactor and the activity of the leached ^{64}Cu was determined in the course of the experiment using a scintillation detector, as shown in Figure 4. A similar study was conducted on Cu ore leaching, in which ^{64}Cu was used as a radiotracer in the hydrometallurgical recovery of Cu with similar properties as the radiotracer [107]. RTD studies of this two-step system were carried out. The experiments indicated a dead volume which was estimated as 15% of the total volume, and the fault was discovered to be the lack of reliable stirrers. The radiotracer–RTD method was a sufficient tool for troubleshooting and optimizing the leaching system. The study concluded that regardless of the outcome of the leaching yield, an efficient radiotracer technique grounded on the NAA technique was developed for the optimizing and online control of the process. This is because the outcome of NAA was confirmed by the ICP-MS analysis [107]. The studies showed that the radiotracers could give robust results in hydrometallurgy in the optimization of the processes.

3.3. Application of Radiotracers in Solvent Extraction of Metals

In recent years, hydrometallurgical metal recovery methods have become more significant. In conjunction with this tendency, solvent extraction as a technical step has been of great interest in various laboratories globally [108]. A solvent extraction system contains two immiscible solutions encompassing a less polar organic phase comprising the diluents, extractant(s), and a modifier, and a more polar aqueous phase carrying the metals to be separated. However, many solutes may be available in the initial solutions, and extracting system may encompass a combination of solvents made to selectively remove or recover one or more solutes, depending on their chemical properties [109]. Researchers have made efforts to make improvements in the metal separation of the less polar phase through the development of extracting agents, changing diluents, using mixtures of extractants, and adding modifiers [110]. For that reason, solvent extraction is the most efficient technique in the enrichment of metal ions/cations.

The multiple aspects of effects accountable for the phase transition of metal ions give the solvent extraction process a wide range of application possibilities [111]. The inclusion of neutral ligand-generating adduct complexes in the organic media improves the solvent extraction of metal chelates with an excess of coordination sites. This synergistic recovery of d and f- block and (4d/5d in specific) components, especially in a mixture of Lewis and β-diketones bases such as organophosphorus esters, has sparked a lot of attention. The degree of synergism is determined by the qualities of the extractants and the type of solvents used [112]. Species are recovered using a mixture of extractants, with the distribution ratio being higher than the sum of the individual extractant's distribution ratios. The synergistic effect improves not only extraction selectivity and efficiency, but also the stability of the extracted complexes, eliminating the emulsification and creation of the third phase, and boosting the extraction rate [113].

Establishing optimum conditions for the solvent extraction of metals necessitates a significant amount of experimental and theoretical effort. The application of the radiotracers is preferable in the determination of the cation concentration during solvent extraction. That is because the concentration of the metals can be obtained independently in both phases without the application of extra separation procedures [111]. The sensitivity can be accustomed in an extensive range of procedures, depending on the needs of the specific activity. With radiotracer-labelled reagents, it is possible to obtain details on the distribution behavior of diluents and extractants. Such information is required for the quantification of extraction reactions. The implementation of the tracer approach is the preferred way of determining fundamental reaction parameters and technical characteristics in the formulation of liquid–liquid extraction processes. As is widely known, the approach has a high detection sensitivity and saves time, especially in continually functioning equipment. Variations in processing conditions, such as pH, concentrations, temperature, and so on, have a minor impact on the outcomes. The primary need for a radiotracer is that it behaves identically to the nuclides it describes. It must also have a long half-life and be a gamma-

emitter to make detection easier [114]. Another benefit is the ability to designate the main and contaminated metals and determine their distribution behavior. For instance, when the manufacture of ^{14}C-labelled compounds is feasible, it is also feasible to estimate the distribution of extractants and diluents in a straightforward manner [111].

The knowledge of the radiotracer has been applied in the exploration procedures in the solvent extraction of a few metals. That could be attributed to the availability of only few facilities for generating radionuclides. Additionally, the knowledge and acceptance of radiotracers in various industries and research fields are still low. That indicates that there is a gap that needs to be explored through the application of radiotracer approaches in hydrometallurgy due to the sensitivity and reliability of the method. Some of the metals that have been explored using the radiotracer technique include Cu, Pt, Au, Zn, Cd, Ag, Fe, In, Co, and Eu and others are addressed in the subsequent sections.

The application of hydrometallurgical processes in Cu production has matured tremendously [115–117]. Cu is a strategic metal that forms a very important role in transitioning to renewable sources of clean energy. Thanks to the use of hydrometallurgical processes, the recovery of this metal would be possible because this method enables the recovery of even trace amounts of metals from ores [107]. The extraction process can be chosen for the selective separation of Cu from multi-element pregnant leach solution (feed solution), due to its positive economic and environmental aspects, and high efficiency of the process. The active extractant compound of the ACORGA P50 is 5-nonylsalicylaldoxime (2-hydroxy-5-nonylbenzaldehyde oxime) can be used in extracting Cu and the recovery effectiveness can be analyzed using a ^{64}Cu radiotracer. One stage of the extraction process is enough for the achievement of almost 100% yield of the selective Cu^{2+} recovery from the aqueous feed solution. The selective extraction of Cu^{2+} with ACORGA P50 extractant increases with pH value, reaching the highest yield in the range of pH = 1.2 for the initial concentration of the extractant in 2.5% vol. kerosene [51,107].

In the modern world, the group of REEs such as Eu has gotten a lot of interest [118,119]. The usage of Eu and other REEs in future sustainable operations, such as reliable lighting and green energy sources such as wind turbines, has raised the need for these metals worldwide [119]. The most common process for separating REEs is hydrometallurgy, which encompasses leaching, precipitation, and solvent extraction [118]. Various types of solvents can be used in conjunction with the radiotracer technique for the selective recovery of Eu. Some of the already applied solvents in extracting Eu are organophosphorus acids (H_2A_2, dimer); ethyl hydrogen benzyl phosphonate (HEBP), trifluoroacetyl-pyrazolin-5-one (HPMTFP); and a synergic solution of crown ethers (benzo-15-crown-5, 18-crown-6, 15-crown-5), HPMTFP, and dichloromethane (DCM) [120–122]. The retrieval of Eu^{3+} from aqueous perchlorate solution using ethyl HEBP solubilized in organic solvents of various dielectric constants from aqueous perchlorate solution at a constant ionic strength of M = 1 (Na^+ $HClO_4$) and a pH of 2.5 at various temperatures was studied [121]. The radiochemical quantities of Eu in both phases were obtained by measuring the activities of ^{152}Eu and ^{154}Eu using a Na(T1) scintillation counter (ECKO). The ratio of the radioactivity in the organic phase to the one in the aqueous phase was used to calculate the metal's distribution ratio (K_D). The equilibrium constants were found to drop in the following order: n-hexane > carbon tetrachloride > nitrobenzene > benzene > chloroform > benzene > chloroform. The study results revealed that the nature of the pH, solvent, and HEBP concentration all have a significant influence during the extraction of Eu^{3+} by HEBP [121].

Apart from Eu^{3+}, Lu^{3+}, and La^{3+} some of REEs play a crucial role in the current world. La is utilized in the production of carbon arc lights, which are employed in the film industry for projector lights and studio lighting, and in making glass applied in camera lenses and other special glassware, among other purposes [123]. On the other hand, Lu compounds are employed as hosts for X-ray phosphors, and scintillators and their oxides are applied in optical lenses [124]. Consequently, Lu and La are critical minerals for modern-world technology and their separation and recovery are important. Tracking the method of the in-situ chelation of Lu^{3+} and La^{3+} in forming a solid matrix is feasible through the

application of mixed hexafluoro acetylacetone (HFA) and tributyl phosphate (TBP) as chelating agents, and the use of radioisotopes ^{177}Lu and [140]La as radiotracers [125]. As soon as the polar modifier methanol was introduced to CO_2, the selection of a robust restrictor was shown to be particularly critical for the in-situ chelation of metal ions or organometallic compounds. To achieve the quantifiable retrieval of metal chelates, it was important to optimize the alignment and placement of the output valve and the orientation of the extraction apparatus. Using the radiotracer, the online back-extraction enhanced metal ion retrieval, reduced restrictor clogging, and eradicated the requirement for an organic trapping solvent using this novel method. The reproduction of ligands was enabled through online metal ion recovery, allowing CO_2-containing ligands to be reused devoid of depressurizing the system [125]. Such approaches are employed due to the scarcity of the mineral of interest from their ores and other sources (Figure 5).
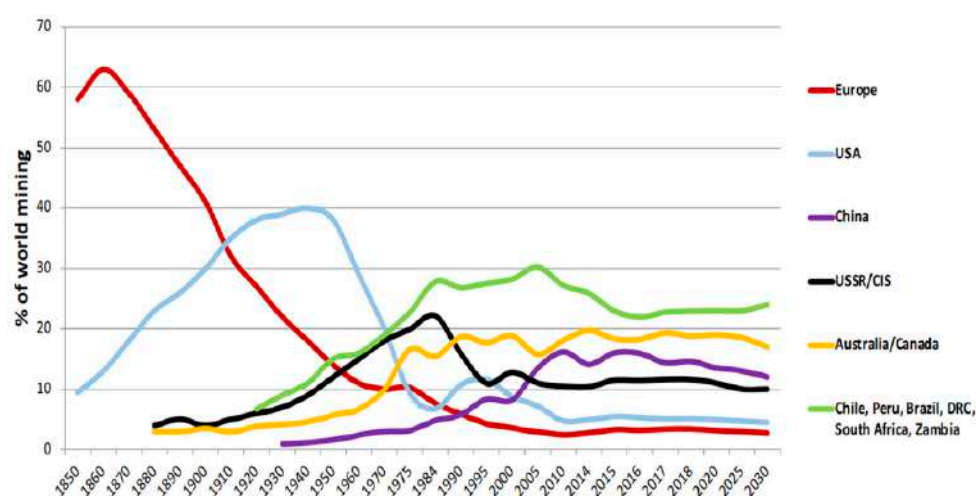
Figure 5. The status and projection of the global mining industry from 1850 to 2030 (metals and industrial minerals as a % of total global excluding coal) [126].

The reason for the scarcity of minerals is attributable to intense mining activities, and metals have significantly reduced in ores, and they exist in low concentrations but are critical for the economy; for instance, Platinum Groups Metals (PGMs) are critical in the green economy [127,128]. Pt is one of the PGMs employed in fuel cells as a catalyst to efficiently convert hydrogen (fuel) and O_2 into heat, water, and electricity [129]. Since the advent of Pt-containing catalysts in automotive exhaust systems, detecting low levels of Pt in environmental specimens has become a major concern [114]. The measurement of precise Pt background concentrations in various materials is necessary to monitor the accumulation of Pt in the environment. Because the amount of Pt in sediment samples is so minimal, creating methods to determine its quantities is incredibly difficult. The most efficient technique to achieve extremely low detection concentrations is to devise a procedure that comprises digestion, separation, preconcentration, and Pt detection [114].

Due to the convenience of tracking [191]Pt activity throughout digestion and recovery, radiotracer procedures would be instrumental in optimizing extraction techniques [114]. The extraction dynamics of Pt^{4+} from an HCl medium using rubeanic acid in TBP, thenoyltrifluoroacetone (TPA), tributyl phosphate, and n-butyl alcohol-acetophenone were investigated using [191]Pt radiotracer [114]. The influence of acidity, shaking time, Pt concentration, and back-extraction were investigated, and it was found that TBP and TPA extraction results were the best when using 4 M HCl and 3 M HCl, respectively. At such concentrations, the maximum levels of the [191]Pt were recovered by the extracting agents. As extraction and back-extraction were conducted twice, the overall recovery of [191]Pt increased. Generally, the extraction with TBP and back-extraction with 2 M NH_3 yielded over 90% [191]Pt removal

from solutions both with and without a substrate. The molar concentration of the NH_3 solvent appeared to have no effects on the back-extraction from TBP. When isotope dilution is used, this recovery is reasonable because any losses throughout the technique are compensated for. Due to the inadequate back-extraction with NH_3, the total recoveries with TBP + rubeanic acid are unsuitable for determining [191]Pt at trace or ultra-trace concentrations [114]. Additionally, the residue of the acids employed for sample digestion reduces Pt recovery with TBP.

The rising industrial consumption of PGMs drives up the utilization of high-grade PGM ore. The rising scarcity of high-grade PGM ore has led to a reliance on low-grade ore. Unfortunately, the expense of extracting PGMs from low-grade ore is prohibitively costly and raises serious ecological concerns. Despite research into the use of fungible substances to partially substitute the usage of PGMs in items such as vehicle catalysts, the net demand for PGMs remains high because of their rising consumption in automobile engines [130]. Every year, approximately 65% of Pd, 45% of Pt, and 84% of Rh are used in catalytic converters to reduce hazardous emissions from vehicles. With stronger pollution standards in place, the fast growth of the new-energy automotive sector will place a greater strain on PGMs supply [130]. Conversely, PGMs in wasted catalysts from a large number of obsolete automobiles must be appropriately recovered. It is possible to follow the solvent extraction of Pd by the radiotracer method. [109]Pd has a short half-life of 13.7 h and its gamma spectroscopy can be studied using scintillation detectors [131,132]. The Institute of Nuclear Chemistry and Technology, Warsaw, developed a scheme for recovering both Pd and Au from electronic waste (Figure 6). The radiotracer was used in monitoring the extraction of Pd in a separating funnel using a fraction of crude oil (H_2S), while diethyl malonate was employed in extracting Au. That was feasible through the application of the distribution ratio (K_D) of the activities of [109]Pd and [198]Au in the organic phase against the aqueous phase, as shown below:

$$K_D = \frac{\text{Radioactivity in organic phase}}{\text{Radioactivity in aqueous phase}} \tag{2}$$

The study concluded that crude oil and diethyl malonate can be used in the selective extraction of Pd and Au, respectively, from electronic waste. The K_D of [109]Pd and [198]Au is very useful in tracking their recovery processes. The developed method of hydrometallurgical and pyrometallurgical separation of Au and Pd was found to give high purity and yield of the elements of interest.

Radiotracer approaches can also be applied during the extraction processes of precious metals known to be vital in various industries [133]. Precious metals such as Au have attracted huge attention in matters of recovery, with different scholars aiming to apply radiotracer techniques in qualitative and quantitative analysis. A normal cell phone contains about 0.02 g of Au. If all of the Au in iPhones sold in 2013 were taken from a single mine, it would leave a gap the size of a six-kilometer-long highway [134]. This example provides a low-level view of the number of resources needed to produce the commodities with which we associate ourselves. Such a level of demand cannot be sustained in the long run if it is exclusively based on resource recovery from rocks. Therefore, other sources need to be considered as part of the circular economy, and their recovery can be optimized using modern techniques such as radiotracers [51,135].

As public concern about the environmental implications of cyanidic Au extraction has grown, the creation and application of alternative hydrometallurgical extraction procedures have become a priority for many research institutions in recent decades. Employing [198]Au radiotracer technologies, a study was carried out to measure the retrieval of gold moving from the sample into the Cu-matte and its depletion with a waste slag [65]. The radiotracer technique was based on the chemical balance of the tracer [198]Au put into the process with a single Cu source. Labeled minerals and concentrates were used in the experiments. Chloroauric acid ($HAuCl_4$) was used to plug the holes in mineral scraps. The metallic [198]Au absorbed in the scrap was the residue after the evaporation to dryness. Following

the introduction of the tracer into the shaft furnace, waste slag and Cu-matte samples were collected. A lead-shielded NaI(TI) detector, 50×50 mm in size, was then used in conjunction with a single-channel analyzer for the measurements. The quantification was conducted using the total count rate of the tracer traveling from a specific source to the sampled product [65]. The overall count rate (cps/N) of the tracer passing from a specific source to the sampled product was computed using Equation (3).
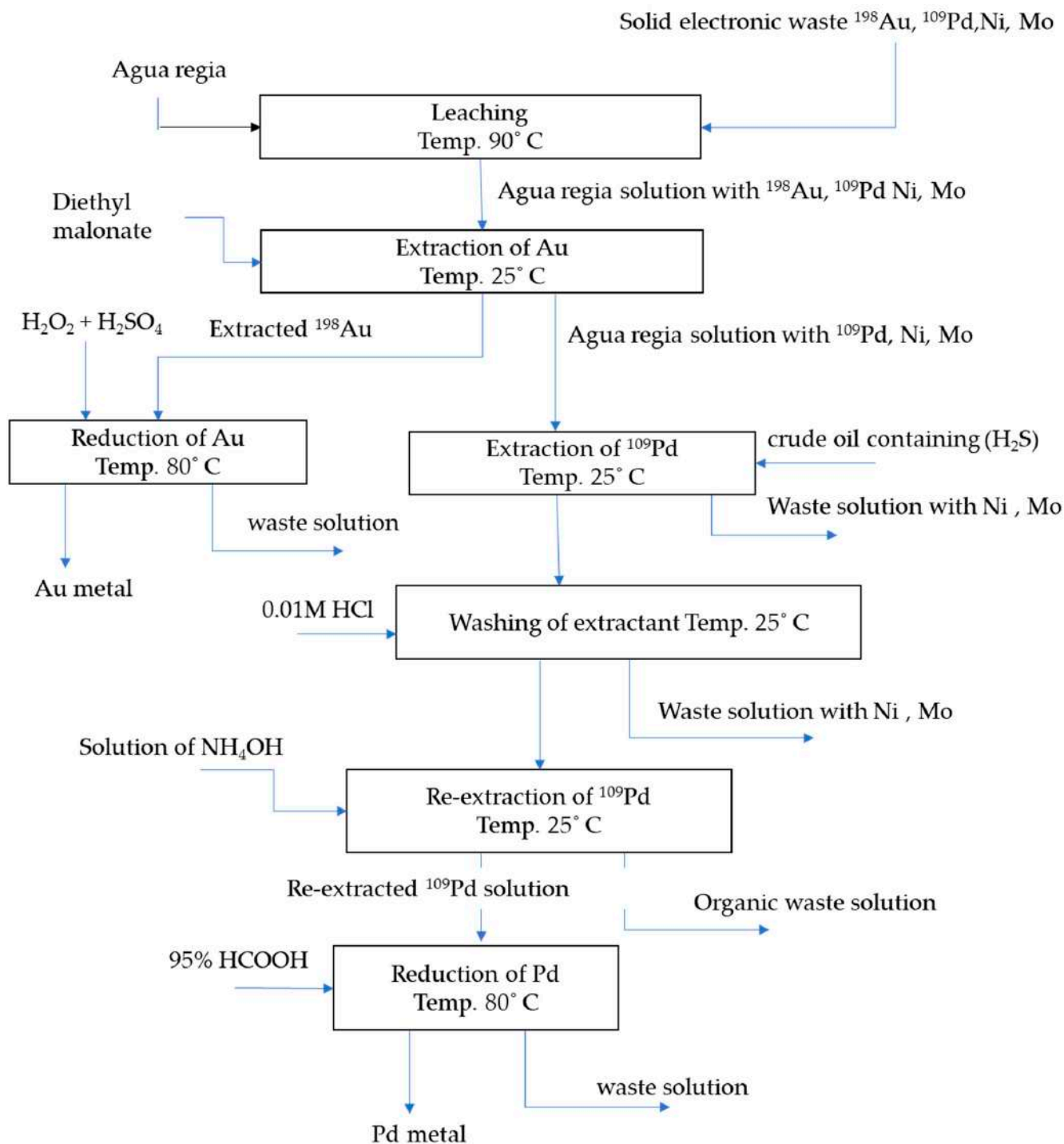

Figure 6. The scheme shows the separation of Pd and Au from electronic waste using the radiotracer technique.

$$N = \frac{M}{t_2 - t_1} \cdot \int_{t_2}^{t_2} 1/t/dt = \frac{M}{t_p} \cdot \sum_{i=1}^{n} I_{1/t/} \cdot \Delta t \tag{3}$$

wherein M is the mass of the gathered material/slag/Cu-matte (kg); t_p is the period (s) of the "radiotracer cloud"; $A_t = t_{i+1} - t_1$ is the time interval of sampling represented as $\Delta t = 5$ for slag sample and $\Delta t = 1$ min for Cu-matte. The time interval t_p in this formula is the effective material discharging period from the sedimentation tanks, adjusted for interruptions in the discharge of slag or Cu-matte. Tracer activity (A) was found to be equivalent to cumulative count rate (cps) and it was determined by applying Formula (4):

$$R = \left\{ 1 - \frac{A_S}{A_0} \times 100\ \% \right\} \tag{4}$$

whereby $A_0 = A_s + A_m$ was the cumulative activity of the injected tracer which was equal to the activities acquired in slag and Cu-matte, respectively. The study demonstrated that the activity from the metal of interest can be used in quantifying its amount in a specific material at a specific time.

The separation and quantification of the Au can also be actualized by applying solvents such as β-diketones (benzoyl acetone (BZAC) and thenoyltrifluoroacetone (TTA)) [112]. The research was conducted utilizing the [198]Au radiotracer technique to investigate the recovery of Au^{3+} using the two abovementioned β-diketones and the enhancing impacts of tri octyl phosphine oxide on such extractions in several organic solvents [112]. Following equilibration, two phases were isolated, and the radio-activities of equal quantities (1 mL) of each phase were measured. Distribution coefficients (K_D) were computed from the earlier outlined Equation (2).

The distribution coefficient (K_D) is a crucial parameter in monitoring the transfer of the cations from one phase to another. The addition of the organophosphorus compound (TOPO), which had no extraction abilities for Au, increased the distribution coefficient (K_D) of Au^{3+} recovered with a fixed amount of N-(thioacetyl)-benzamide (HA) (TTA or BZAC) [112]. That was attributed to the creation of a more lipophilic adduct with the donor. In chloroform (BZAC chelate) and carbon tetrachloride (TTA chelate) conditions, a powerful ternary adduct complex creation was observed. The influence of temperature changes created spontaneous, enthalpy-favoring processes with a net entropy loss. The diluent dependence of synergic effects was recorded, and Hildebrand's regular solution theory was discovered to be appropriate in such schemes [112].

The concept of the radiotracer can be applied in the solvent extraction of Au from jewelry wastes. Figure 7 shows a block diagram of the developed technology at the Institute of Nuclear Chemistry and Technology for Au extraction using the radiotracer technique. The method is particularly helpful in examining extraction parameters such as the extraction coefficient and equilibrium time. Such parameters can be determined using radioactive isotope [198]Au [136]. An aqueous solution (aqua regia containing Au) was labelled with [198]Au, while diethyl malonate was utilized as an extractant. Marker [198]Au was obtained by irradiating high-purity metallic gold in a nuclear reactor preceded by the dissolution of the sample in a small amount of aqua regia. The extraction process for the change of parameters was carried out in a separating funnel. The phases were then separated, and samples were taken from each phase for radiometric measurements using a germanium/lithium/semiconductor detector. Given the number of counts in the relevant phases, the basic parameters of the extraction process can be calculated in a simple way using the formula below:

$$E = \frac{I_O - I_t}{I_W - I_t} \tag{5}$$

where;

- E is the extraction coefficient;
- I_0 is the number of counts in the organic phase of volume V;
- I_w is the number of counts in the water phase of the same volume V;

— I_t is the background of the measuring device.

$$\%E \;=\; \frac{100\,E}{\dfrac{V_0}{V_W} + E} \tag{6}$$

Using the technique of isotope tracers, the equilibrium time and the capacity of the extractant under equilibrium conditions can be determined. The approach can recover high-purity Au with a high yield.
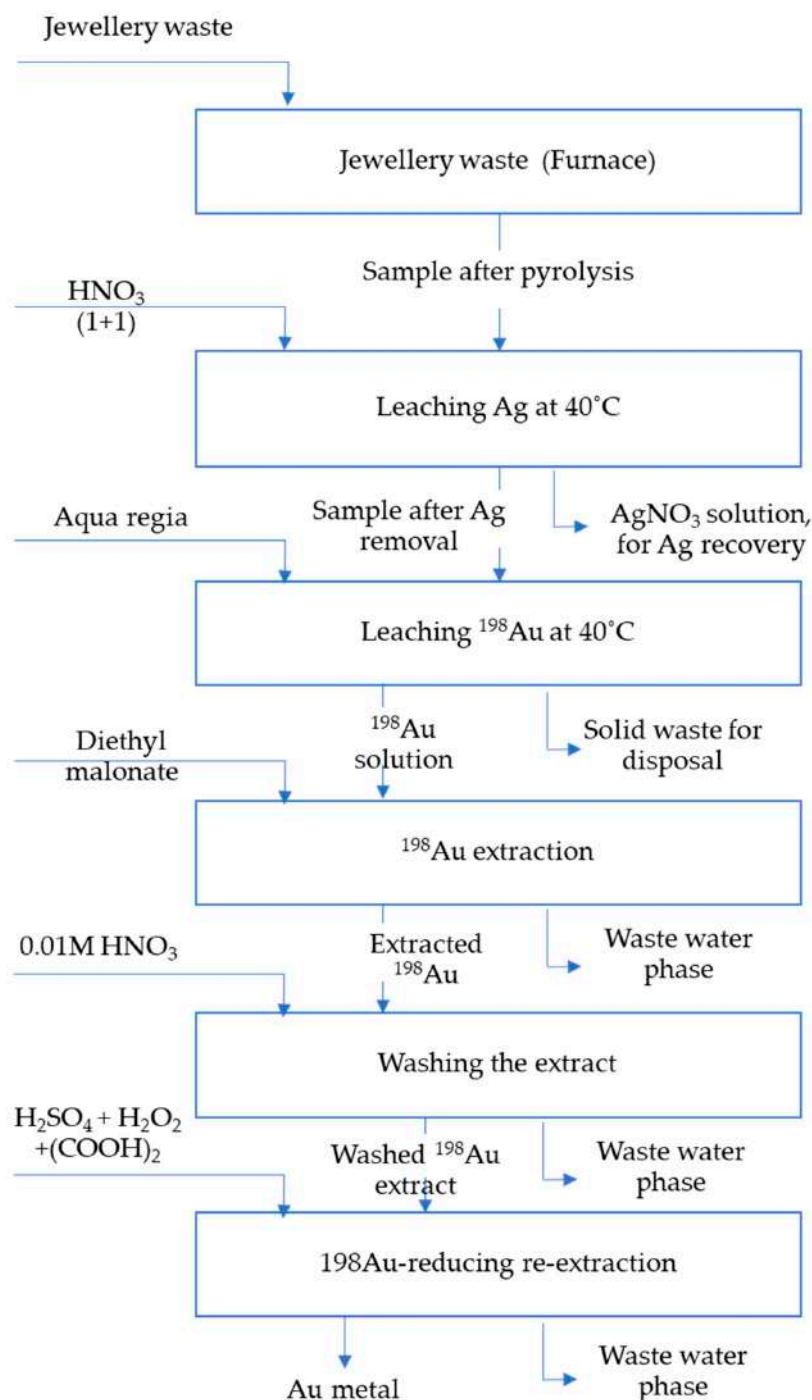
Figure 7. Au recovery from jewelry waste.

In a comparative study, ^{198}Au was used to explore the removal of Au^{3+} from an aqueous acidic media [137]. N-(thioacetyl) benzamide in chloroform was employed under the influence of organophosphorus donors (tributylphosphine oxide (TBPO), tributyl phosphate, and triphenylphosphine oxide) at pH 3.0 [137]. The degree of ^{198}Au^{3+} extraction in the binary complex increased with the temperature, but the ternary complex showed the opposite phenomenon. When the organophosphorus compound was added to ^{198}Au^{3+} extracted with HA, the distribution ratio increased. That was linked to the creation of a more lipophilic adduct with these donors [112,137]. In the experimental temperature range, all of the thermodynamic functions of the synergistic extraction procedure tended to be negative. The negative enthalpy estimates for adduct development indicate that the adduct comprising TBPO possesses the most advantages of the three donor systems, which is consistent with the phosphoryl oxygen atom's electron donor power. The stronger the donor power, the more likely it is that a new bond will form with the gold atom. Because the generation of adducts is not preceded by bond breakage, a negative enthalpy change is anticipated [137].

Likewise, the solvent extraction of KAu(CN)$_2$ from alkaline cyanide solutions was evaluated using a ^{198}Au tracer through the application of quaternary ammonium tetradecyldimethylbenzylammonium chloride (TDMBAC) as an extractant with the addition of tri-n-butylphosphate (TBP) [138]. Several variables were studied, including agitation time, TBP volume %, and the molar fraction of TDMBAC in the aqueous phase. According to the findings based on the activities in different phases, the organic phase had a high extraction capacity [138]. Almost all of the Au (CN)$_2^-$ (>95%) in the aqueous phase was transported to the organic phase, as signified by a high distribution ratio. The TBP modifier was significant during the extraction process, since almost all ^{198}Au remained in the aqueous phase without TBP. An increase in TBP concentration caused a rise in the extraction percentage when the % volume of TBP was less than 15%. When the ^{198}Au concentration was less than 4 g·L^{-1}, [TDMBA+] · · · [Au (CN)$_2^-$] · · · 4H$_2$O· · ·4TBP was recommended for the generation of a supramolecular microstructure in the organic phase. By introducing the organic phase comprising TBP to the aqueous phase, the complex moved into the organic phase and microemulsion or reversed micelles were generated when the ^{198}Au quantities attained a particular limiting amount. The majority of the ^{198}Au in the organic phase can be stripped out with aqueous solutions of 2,2′-thiodiethanol, ammonium thiocyanate, or glycol, from which elemental Au might be retrieved with the application of reducing agents such as Zn and NaBH$_4$ [138].

In an alkaline cyanide mixture, the liquid–liquid extraction of Au can be monitored by a ^{198}Au radiotracer [139]. Amines tetradecyldimethylbenzylammonium chloride, tri-n-octylamine, and N1923 were some of the extractants utilized in these experiments. The solvents were found to be effective in the removal of Au from the alkaline cyanide solutions [139]. Through the application of K$_D$ based on the radiotracer method, the effects of numerous parameters on Au recovery can be explored, including the molar ratio of extracting agents to Au concentration, % capacity of cosolvent, and the pH value of the aqueous phase. The approach also offers an opportunity to study the recovery behavior of Au or any other metal present in low concentrations in a convenient, quick, and accurate manner [139,140]. From the various examples given on Au extraction, it is evident that the use of isotope markers is prudent in the evaluation of the Au recovery capacities of different solvents.

In addition, precious metals, REEs, and transition metals such as Zn, Co, and In play very crucial roles in the modern economy. For instance, Zn is employed in infrastructure, transportation, electronics, and renewable energy for a low-carbon economy [135,141]. Zn is a vital substance for the future because of its exceptional capacity to shield metals from rust and its expanding involvement in energy production and storage. Zn coatings help preserve and prevent rust on solar panel fittings, and wind turbines need a Zn covering/paint to withstand harsh weather conditions. Its recovery process using approaches such as solvent extraction is, therefore, important.

Sample diagrams of the technological recovery of strategic metals from various waste products of the electronics industry were developed at the Institute of Nuclear Chemistry

and Technology, Warsaw, and are shown in Figure 8. To determine the possibility of the selective separation of Zn, Mn, and Mg from spent Zn electrolytes, research was carried out. The extraction of these metals was conducted using two-diethyl hexyl phosphoric acid (D_2EHPA) diluted in n-heptane. Using ^{65}Zn and ^{54}Mn radioisotopes as markers, the extraction of the metals from the sulphate solution containing 15.9 g/dm^3 of Zn, 0.89 of Mn, and 24.3 g/dm^3 of Mg was investigated. The study concluded that the extraction equilibrium was attained after 4 min for both ^{65}Zn and ^{54}Mn, during which the selectivity of the extraction was controlled by pH variation.
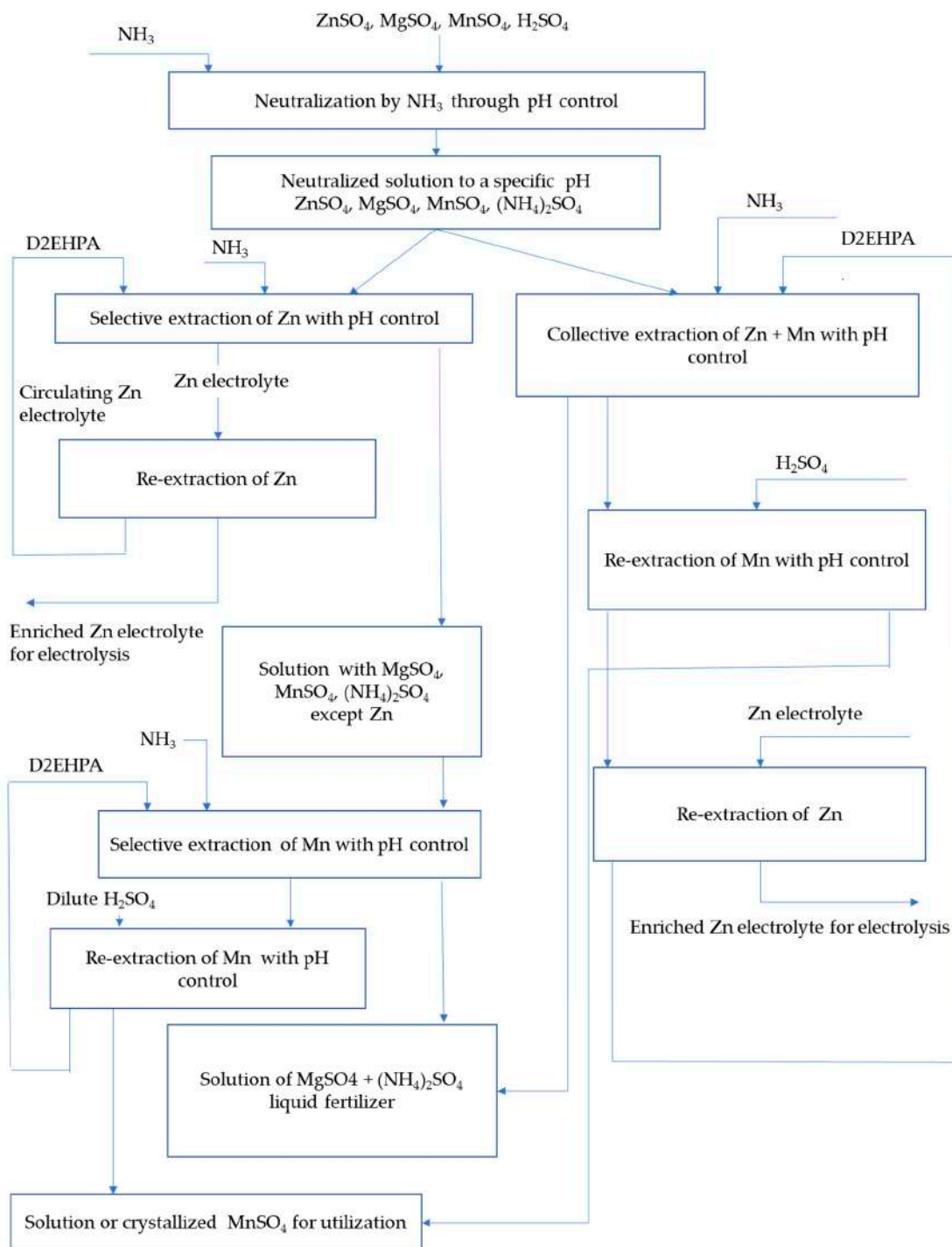

Figure 8. Flowsheet demonstrating the extraction of Zn and Mn from used Zn electrolyte waste.

Due to the improvements in hydrometallurgical technologies, a radiotracer technique was also applied to compare different phases of separation, extraction, and back-extraction [111]. Cd and Zn were isolated from Co using liquid–liquid extraction from a chloride mixture comprising sixteen distinct metal ions. The distribution of such cations in the different phases of the extracting agents indicates the capacity of such solvents to recover the metals of interest. The distribution ratio (K_D-ratio) can be represented by Equation (7):

$$K_D = \frac{M_{org}}{M_{raf}} \tag{7}$$

where M_{org} is the analyte concentration in the organic phase and M_{raf} is the total amount of the cation/analyte in the aqueous phase. During the radiotracer analysis, liquid scintillation spectroscopy was applied in the measurements of the concentration of ^{109}Cd radiotracer in the solutions. However, a High-Purity Germanium detector (HPGe) was applied in the analysis of ^{65}Zn with a characteristic energy line at 1115 keV, while ^{60}Co showed peaks at 1173 keV and 1332 keV, respectively. The lowest difference between raffinate and feed that may be measured determines the lowest feasible K_D ratio [111,142]. The investigation also revealed that single-phase analysis conducted using the ICP-MS had a greater K_D ratio compared to the two-phase assessments conducted using radiotracers. When considering extraction mechanisms and speciation, ICP-MS measurements should be utilized with caution, as they usually require the analysis of extraction curves obtained from extremely low and high K_D values [111].

Such evaluation on the transition metals has been extended to recovery studies regarding Fe, which is crucial in the global economy [143]. It is part of a wide group of minerals known as ferroalloys, which are used as additive agents in steel production. It is also a key component of many special-purpose alloys designed for electrical resistance, magnetic properties, heat resistance, thermal expansion, and corrosion resistance [144]. Despite the invention of other resources, Fe and its alloys continue to play an important role in the economics of modern countries, making it a crucial mineral that requires the optimization of its recovery.

Fe^{3+} removal from aqueous acidic solutions by liquid–liquid extraction has received a lot of attention in recent decades. Using the radiotracer technique, the behavior of Fe^{3+} extraction from an aqueous chloride solution using 2-hydroxy-N-phenylbenzamide (HA) in n-butanol under the conditions of numerous organophosphorus donors such as triphenylphosphine oxide, trioctylphosphine oxide, and TBP at pH 2.0 was examined [113]. Fe^{3+} was spiked with ^{59}Fe in the presence of this chelating neutral and reagent organophosphorus compounds such as TOPO, TBP, and triphenylphosphine oxide (TPPO). With the addition of various organophosphorus chemicals, the distribution ratio of the extracted Fe^{3+} was found to increase with HA [113]. The study also discovered that the extent of Fe^{3+} absorption into the organic phase increased with temperature, both as the binary complex [$FeA_2Cl (H_2O)$] and as the ternary complex [$FeA_2Cl(S)$]. The neutral donor's synergistic impact is due to the replacement of the coordinated water molecule from the metal's primary coordination sphere. The findings from a study of the synergistic effect of organophosphorus donors on the chelating extraction of Fe^{3+} in an organic solvent is promising for hydrometallurgy [113]. Besides solvent extraction, adsorption is another key technique that can perform a vital role in the recovery of metals.

3.4. Application of Radiotracers in the Adsorption Processes of Metal Recovery

Adsorption is the process by which a metal ion (adsorbate) moves from a solvent phase to create a thin monomolecular layer on a liquid-condensed phase (substrate) or solid phase. The hydrometallurgical recovery of the various cations is increasingly evolving with the application of radiotracers in examining various adsorption/sorption processes [145]. Methods such as the use of Solid-Phase Extractants (SPEs) in hydrometallurgy have the benefits of high separation efficiency, low Volatile Organic Compounds (VOC) inventory, and the capability to work in the column mode [146]. The adsorption of cations by various

surfaces is generally mentioned as a preferable method for metal ion recovery compared to other hydrometallurgical approaches because of its effectiveness, simplicity, suitability for batch versatility, application at very low concentrations, and continuous operations, limited sludge creation, ease of operation, low capital cost, and potential for regeneration and reuse [147]. Dead biomass, polymers, clay minerals, and metal oxides are some of the surfaces that have attracted huge attention for their consideration as adsorbents for cation recovery when coupled with diverse extractants [148]. Critical metals such as REEs, transition metals, and some actinides can be recovered from various environmental sources such as ores, mining waste, radioactive wastewater, seawater, and freshwater.

Numerous actinides, lanthanides, and transition metal ions/radiotracers are proven to have strong adsorptive characteristics, leading them to bind not just to mineral particles, but additionally to colloids and natural organic materials, boosting their bioavailability and migration. High-affinity sorbents may capture ultra-trace and trace amounts of actinide and lanthanide from aqueous environments, and they have a variety of useful functions [148]. Because of their potential to absorb and concentrate large amounts of ultra-trace level species, such substances are great candidates for emerging pollution control techniques and crucial material recovery operations. The efficient reclamation of minute concentrations of actinides, lanthanides, and transition metal ions is beneficial for mineral recycling and recovery, chemical separation, in situ monitoring, and environmental remediation.

Radiotracers have been used in several studies exploring the cations' separation/recovery by various adsorption materials defined by diverse properties and abilities. An investigation used isotopic radiotracers to determine the capacity of several ordinary and nanoporous sorbent materials to extract and remove specific actinides (Th, Pa, U, and Np) and lanthanides (Ce and Eu) from salt and freshwater systems [149]. To a sorbent/water mixture, a small aliquot of each tracer standard solution was added, in which a sorbent to liquid ratio of 1 g/L was used uniformly, with the exception of U, in which case this ratio was lowered to 0.2 g/L. Gamma counting on a low-background, high-efficiency High-Purity Germanium (HPGe) detector was then used to determine the activities of ^{139}Ce, ^{233}U, ^{155}Eu, ^{234}Th, ^{237}Np, and ^{233}Pa in different phases. However, the activities for ^{233}U were assessed using a Beckman Coulter LS 6500 and EcoLume LC fluid as Liquid Scintillation Cocktails. Each analyte's activity was utilized to calculate a mass-weighted distribution coefficient (K_D, L/kg) as per Formula (8), below:

$$KD = \frac{A_S}{A_W}\frac{V}{M} \tag{8}$$

whereby A_S denotes the total activity of the isotope captured in the sorbent, A_W is the total activity that remained in the mixture, V represents the batch experimental volume in liters (L), and M is the sorbent mass (kg). The $K_D > 10^4$ (log $K_D > 4$) suggested relatively strong affinity sorbents were successfully kept in collector columns. The study reported that the nanostructured composites outperformed conventional materials in terms of consistency and performance. In both sea and river water, a nanoporous silica surface treated with 3,4-hydroxypyridinone exhibited excellent recovery and uniformity abilities [149]. Additionally, MnO_2 materials, particularly the high-surface area small-particle material, showed good recovery performance [149]. This implies that the radiotracer techniques can be employed in the assessment of hydrometallurgical separation and recovery of lanthanides and actinides from water bodies.

The trivalent lanthanides and actinides form the most complex elemental separations on the periodic table. That is because they have similar chemical and physical properties [47,150]. Due to their regularly ordered mesopores, high surface areas, low reactivity, large pore volumes, tunable pore size and morphology, thermal and mechanical stability, and potential for surface functionalization, Ordered Mesoporous Carbon (OMC) materials are an appealing alternative to the conventionally used polymeric resins in the recovery of such elements. The ability to use OMC composites for metal ion/radiotracer separations might have huge benefits because the smaller particle size limits the longitudinal

diffusion of a specific analyte and boosts the number of theoretical plates in a specific column predicated on such matrixes, thus further enhancing the separation resolution. The increased surface area of the OMC allows greater ligand loading performance. Given the persistent complexity of intragroup, trivalent lanthanides, and actinides separations, and the anticipated increases in resolution and loading capacity of OMC materials, using such composites to accomplish lanthanides and actinides separations is a natural next step [150]. Because of their small mesh size and consistent shape, OMC composites are suitable candidates for recovering the neighboring REEs. The hydrometallurgical performance of such surfaces can be evaluated using radiotracer techniques.

For instance, a $^{152/154}$Eu^{3+} isotope marker as a representative of REEs in 0.001 M HNO$_3$ was incorporated into the aqueous phase at 25 °C and agitated at 1500 rpm for 30 min while in contact with LN resin or OMC materials [150]. Following contact, the samples were centrifuged for fifteen minutes, and transfer pipettes were utilized to collect the aqueous phases from the LN Resin, while 0.2 μm syringe filters were employed to extract the aqueous phases from the OMC components. For gross gamma counting, a 200 L fraction of each aqueous phase was obtained for the computation of distribution coefficients for each sample using Equation (9):

$$K_D = \frac{A_0 - A}{A} \frac{V}{M} \tag{9}$$

where A_0 and A are the aqueous phase's activity (counts per minute/CPM) before and after equilibration, respectively, while V is the aqueous phase's volume (mL), and M is the solid phase's mass (g). Larger K_D values indicate more sorbent material sorption ability for Eu^{3+} [150]. The K_D value for all materials reported decreased as the concentration of HNO$_3$ increased, and throughout all HNO$_3$ concentrations, both the di-(2-ethylhexyl) and phosphoric (HDEHP)-OMC matrix had a greater K_D value than LN Resin. Because all of the polymers employ HDEHP as an extractant, the greater distribution factors may indicate that the larger surface area of the OMC nanoparticle sorbents contributes to $^{152/154}$Eu^{3+} absorption [150]. The HDEHP-OMC composites outperformed current state-of-the-art nanomaterials in terms of distribution ratios and loading capabilities. A separation of Eu^{3+} and Nd^{3+} was accomplished utilizing a tiny and unpressurized column, which demonstrated the criticality of the radiotracer method in due course [150]. The study concluded that EHP-OMC demonstrated its viability as a solid phase sorbent for chromatographic lanthanide and intragroup separations.

The process/behavior of adsorption of Nd (REE) from aqueous systems can also be conducted using the clay minerals montmorillonite, zeoliferous rock, and kaolinite at 27.5 ± 0.5 °C, using ^{147}Nd-labeled solutions with concentration ranges of 10 to 450 mg L^{-1} [151]. The Nd adsorption analysis was conducted in a thermostated bath by agitating 100 mg of the particles with 10 mL of the respective ^{147}Nd-labeled treatments. Following the treatment, the solutions were swirled at 3000 rpm for 30 min, and a particular amount of the clear resulting liquid was quantified in a well-type (3″ × 3″) NaI (TI) detector linked to a standard γ-ray spectrometry configuration. The uptake of ^{147}Nd was estimated by subtracting the initial and final count rates [151]. The sorption isotherms for ^{147}Nd produced for the three core samples revealed that montmorillonite has the greatest absorption ability, with a Cation Exchange Capacity (CEC) of 108 meq/100 g. Nevertheless, based on the materials' CEC, the theoretical yield of ^{147}Nd sorbed by the zeoliferous and montmorillonite rock samples in the examined concentration range was rather minimal. This is because of the difficulties of replacing the Ca-cations of montmorillonite and the exchangeable cations contained in the mineral deposits of the zeoliferous rock with ^{147}Nd-cations [151]. Such studies were conducted several years ago, followed by other similar investigations on different metal ions using distinct surfaces.

Generally, sorption-based surfaces have continuously been invented to study the adsorption behavior of different critical cations in the periodic table. Synthetic zeolite (Z and YZ) and natural (clinoptilolite) composites with polyacrylamide (PAAm) are some of

the other materials developed for the cation adsorption processes. The sorption properties of minerals for these surfaces and their materials were examined for Tb counterparts to REEs using the isotopic tracer technique, with ^{160}Tb functioning as the radiotracer. Tb^{3+} was chosen to represent the REEs (lanthanides) with comparable physicochemical characteristics, with the benefits of ^{160}Tb being its high natural availability (100%), relatively short half-life (72 days), and high cross-section for the thermal neutron capture ($\alpha = 25.5$ b) of its precursor. Tb, like the other lanthanides, is essential in the industry; it is utilized in cathode ray tubes, optical computer memory, magnets, and other applications. Aside from economic considerations, the recovery of REEs is critical due to their toxicity and radioactivity with respect to nuclear waste [147]. The system used to remove Tb was a hybrid of PAAm and Z or YZ, whereby the Tb sorption capabilities were greater than those of plain Z and YZ as per the estimated percentage transfer using Formula (10), below:

$$F = \frac{A_i - A_e}{A_i} \tag{10}$$

wherein A_i and A_e are the activities recorded in the standard and equilibrium solutions, respectively. The radio-activities were used to compute the percentage transfer (F) of ^{160}Tb to solid phase from Tb^{3+} mixtures. The adsorbed quantities (mol kg^{-1}) were estimated as Q = [FCiV/w], where Ci is the initial Tb^{3+} content (M), w is the adsorbent mass (kg), and V is the volume of the solution (L). Because PAAm is neutral, Q values were established using the Z and YZ components of sorbent materials (0.035 g of 0.1 g PAAm-Z/YZ) [147]. The reusability studies for the complexes revealed that the material may be regenerated once the loaded ion was completely recovered. PAAm-Z, unlike PAAm-YZ, was tolerant to acidic environments and the combined findings from the radiotracer analysis indicated that the PAAm and Z composite is a potentially cost-effective material for Tb^{3+} and REEs [147]. Therefore, the materials can be utilized on industrial and laboratory scales for the recovery of such metal ions from numerous sources.

During the exploration of the elimination/extraction of Ce^{3+} ions from aqueous media by a well-defined hydrous ferric oxide (HFO), an isotope tracer was applied [148]. The adsorption tests were carried out by periodically agitating and equilibrating 0.1000 g of HFO in 10.0 cm^3 of the required level of labelled adsorbing solution of Ce^{3+} [148]. The equimolar mixture was then agitated for phase separation before being examined for β-activity determinations with an end-window Geiger–Müller counter. However, the radioactivity of some samples was also tested for γ-activity using a Multi-Channel Analyzer [148]. The sorption ability of the material was examined using the distribution ratio (K_D) indicated below in Equation (11):

$$K_D = \frac{\text{Radioactivity absorbed/g of adsorbent}}{\text{Radioactivity of equilibrat ed solution/mL}} = \frac{R_0 - R_e}{R_e} \times \frac{V}{m} \tag{11}$$

wherein R_0 is the adsorbate's preliminary activity, R_e is the activity of the supernatant media at equilibrium, V is the volume of the adsorptive mixture (mL), and m is the adsorbent mass utilized (g). For the radiotracer analysis, the concentration of the adsorbents (10^4 to 10^8 mol dm^{-3}), temperature (303 to 333 K), and pH (ca 4.0 to 10.0) were analyzed to determine the best parameters for Ce^{3+} recovery. From pH 4.6 to pH 7.0, the absorption of Ce^{3+} was mild, but after pH 8.0, the adsorption rose sharply because the solid matrix was negatively charged and thus collects Ce^{3+} ions. It was discovered that as the temperature rose, Ce^{3+} absorption enhanced from about 0.446×10^6 to 0.791×10^6 mol g^{-1} at the optimum level [148]. The improvement in cation sorption could be attributed to the amplification of slow sorption phases, transfer against a concentration gradient, formation of novel active sites, and/or diffusion-controlled transport across the energy gap. However, the presence of some cations such as Ba^{2+}, Sr^{2+}, and Mg^{2+} had a negative significant impact on cation uptake by HFO. Otherwise, the irradiation of HFO by a 11.1×10^9 Bq (Ra-Be) neutron source with a neutron flux of 3.9×10^6 cm^{-2} s^{-1} had no appreciable effect on the

degree of Ce^{3+} sorption. As a result, the material was proven to be efficient and could be used to recover Ce^{3+} from various sources, including radioactive waste [148].

Because sorption mechanisms under the influence of humic compounds are thought to be crucial for the distribution, motility, and cycling of actinides and lanthanides/REEs in the ecosystem, there has been a lot of attention paid to this subject in recent years. The impacts of fulvic acid (FA), ionic strength, and pH, on the adsorption and desorption of Yb^{3+} and Eu^{3+} on alumina, were studied using a batch approach using ^{169}Yb and $^{152+154}Eu$ radiotracers, respectively [152]. In the absence or presence of FA, the distribution coefficients for the adsorption and desorption of Eu^{3+} on alumina at pH 4.4, 4.6, and 5.7 in 1 mol/L NaCl systems were measured. The distribution coefficient K_D for $^{152+154}Eu$ and ^{169}Yb in the presence and absence of FA on alumina was computed using Equation (12):

$$K_D = \frac{M}{M} = \frac{V\,(C_0 - C)}{CS} \tag{12}$$

In Equation (9), M and M are the concentration of the solid phase (mol/g) and concentration (mol/mL) of the solution phase, and C_0 and C are the specific activity (CPM/mL) of the treatments before and after interacting with the matrix phase, and V (mL) and S (g) are the volume of solution and weight of alumina, respectively. From the study, it was discovered that FA and pH had a massive impact on the adsorption of $^{152+154}Eu$ and ^{169}Yb radiotracers on the alumina surface. The $^{169}Yb^{3+}$ and $^{152+154}Eu$ adsorption onto a bare alumina substrate proved to be pH reliant but independent of ionic strength. The adsorption mechanism of the hydrolyzable REEs Yb^{3+} and Eu^{3+} does not seem to be purely ion exchange, and the surface hydrolysis paradigm can adequately explain the results on bare alumina [152]. Nevertheless, the impact of FA was FA concentration and pH reliant whereby the sorption of Yb^{3+} and Eu^{3+} was boosted or reduced at different pH ranges when contrasted with FA-free processes. Using radiotracers makes it easy to understand such behaviors by simply using their signals in different phases to track their distribution in different systems. The findings regarding coated alumina could be explained by the interplay between complexations of entrapped FA and dissolved FA with REEs cations [152].

Solid-phase extraction is regarded as an alternate recovery approach to solvent extraction since it can mitigate some of the latter's concerns such as third-phase creation, phase disengagement limits, phase entrainment, and so on [146]. However, SPEs have limited process uses, despite being useful in the laboratory-scale separation of metal ions, particularly when dealing with environmental substances. For the adsorption of trivalent lanthanides (Eu^{3+}) and actinides (Am^{3+}) from a 3M nitric acidic medium, two new diglycolamide-grafted silica-based resins (DGSRs) were utilized [153]. Prior to and after equilibration, appropriate aliquots of the liquid media were obtained for the radiometric assay of $^{152,154}Eu^{3+}$ or ^{241}Am by applying a well-type NaI (Tl) scintillation counter connected to a multichannel analyzer. The K_D of the cations on the resin was determined through the application of Formula (13), below:

$$K_D = \frac{C_0 - C}{C_0} \cdot \frac{V}{W}\ (mL/g) \tag{13}$$

where C_0 and C are the quantities of cations before and after equilibration, W represents the weight of the resin material utilized (g), and V represents the capacity of the liquid media employed (mL). The adsorption of $^{241}Am^{3+}$ onto resin containing one diglycolamide (DGA) moiety (DGSR-I) is far less successful than the adsorption of $^{241}Am^{3+}$ onto a resin containing two DGA moieties (DGSR-II). The maximal uptake of $^{152,154}Eu^{3+}$ (employed as a representation of the trivalent actinide/lanthanide ions) by the DGSR-I and DGSR-II was 13.9 ± 1.3 mg g^{-1} and 10.4 ± 1.1 mg g^{-1}, respectively [153]. Column experiments revealed that the $^{152,154}Eu^{3+}$ breakthrough potential on the DGSR-II column was considerably greater than that found on the DGSR-I column, and effective extraction was possible with a 0.01 M EDTA solvent. The radiolytic endurance of the resins was determined by subjecting the resins to a gamma ray dose of up to 1030 kGy, which resulted in a 50% reduction in K_D

values; at doses of 500 kGy, the K_D values were not affected [153]. The DGA-crafted silica-based resins can therefore be employed to remove trivalent REEs or actinides from extremely acidic waste media because they have excellent radiolytic stability. The study showed that radiotracer technique can be applied in monitoring the adsorption behavior of the cations and, at the same time, can be used to check the stability of the recovery surface in a highly radioactive condition.

In a high-ionic strength environment, the kinetics of a significant number of REEs' adsorption by manganese oxides and iron oxides was examined [154]. Batch tests were carried out at pH 7.8, with varying concentrations of radiotracers of 10^{-9} to 10^{-11} M, which are similar to those encountered in the surroundings. The minerals were mixed with the tracers in solution, and the radiotracer activities were monitored in each phase using a germanium detector connected to an Ortec 7150 multi-channel analyzer. For every isotope, count rates were adjusted for decay during irradiation and measurement time, as well as variations in geometry [154]. Throughout the time-series studies, REE adsorption was provided as percent bound or as partition factors: $K_D(t)$, defined as the concentration ratio of REE in the solid and aqueous media at the time (t). The $K_D(t)$ is a proxy for the thermodynamic partition coefficient ratio K, which is only applicable to equilibrium processes. All phases showed rapid adsorption and high K values (10^5 to 10^7); nevertheless, carbonate complexation had a stronger effect on REE sorption by MnO_2 than FeOOH. Therefore, the radiotracer tests in a carbonate-free solution demonstrated that the rate of sorption of REEs such as Eu by MnO_2 was substantially rapid when carbonate species are absent. FeOOH, on the other hand, only showed a very minimal proportional rate rise [154]. Additionally, the sorption of the lanthanides by FeOOH was found to rely on the ionic and atomic radii, since the atomic radius is known to control the charge density of the metal ion. That influences the coordination chemistry of the components in the medium under study.

3.5. Radiotracer Studies Using Resins

Extensive work has also been conducted over the past decade into the design of extraction chromatographic resins for the separation and preconcentration of cations from the environment for further analysis [155]. Such endeavors resulted in the creation of chromatographic surfaces that allow the efficient, quick, and selective recovery of tri-, tetra-, and hexavalent actinides, and from a wide range of sample forms. Although SPE uses sorbents for neutral particles or ion exchange resins, a form of sorbent predicated on extraction chromatography (EC), in which the organic extractant is intercalated into an inert solid support material, is fast developing as a productive SPE method with extremely impressive outcomes [146].

Uranium (U) is a critical metal in the nuclear industry, and therefore, its recovery is very important for both commercial and ecological protection. The synthesis and characterization of a new-extraction chromatographic resin with the robust adsorption of hexavalent uranyl ion across a broad concentration range of nitric acid and exceptionally high specificity for U^{6+} over Fe^{3+} radiotracers and multiple other cations were reported [156]. The new system (dubbed U/TEVA-2) was made up of a novel liquid stationary phase entailing an equimolar solution of Cyanex 923® and diamyl amylphosphonate (DA[AP]) (available on the market as TRPO (trialkyl-phosphine oxide)) entrapped on Amberchrom CG-71 or silanized silica. The goal was to create a recovery chromatographic resin with markedly increased uranium retention (K_D values) over a greater concentration spectrum of nitric acid and very strong specificity for U^{6+} over Fe^{3+} and other components commonly found in the ecosystem.

The adsorption of radiotracers by the U/TEVA-2 resin from HNO_3 acidic media was determined by combining a measured amount (about 1.00 mL) of a spiked media in a test tube with a fixed mass of resin [156]. The precise ratio of aqueous phase capacity (mL) to resin weight (mg) was changed as needed to induce a noticeable drop in the aqueous phase's activity after a single contact with the polymer. K_D was then computed as the proportion of radiotracer activity in the two phases. Cyanex 923 was found to be superior

to TRPO—Cyanex 925®—because of its low viscosity and improved sensitivity to U^{6+} over Fe^{3+}. It was worth noting that the adsorption of U^{6+} by the U/TEVA-2 resin was greater than 5000 from 0.1 to 8 M HNO_3, as assessed by the K_D values (amount of available column values to peak maximum) [156]. Therefore, the new resin's capacity to highly and preferentially extract U^{6+} from such a vast scope of acid concentrations, combined with its beneficial material characteristics, makes it an attractive candidate for use in the isolation and preconcentration of U^{6+} from the environment.

The possibility of extraction chromatography (EXC) for REEs has also been investigated since it merges the specificity of solvent extraction with the efficiency of ion exchange column procedures. In H_2SO_4, HCl, and HNO_3 solution, the extraction of mixed REEs by N, N′-dimethyl-N, N′-dioctyl-3-oxa-diglycolamide (DMDODGA) and traditional N, N, N′, N′-tetraoctyl-3-oxa-diglycolamide (TODGA) resins were evaluated as a function of acidic concentration [157]. The adsorption of REEs' cations and kinetics were studied in $^{152/154}$Eu at trace amounts of metal-to-ligand ratio (1:50) in HCl and HNO_3 to establish the highest weight distribution ratio values (D_w) achievable without loading implications. For radiotracer assays, the solid–liquid D_w for cations by DGA resins from an acidic medium was evaluated by combining an identified volume (usually 1.0 mL) of a tracer-spiked acidic medium of optimum quantity with a fixed mass of the sorbent (2025 mg). The REE source quantities were varied to obtain equimolar REE concentration and surplus REE concentration, which correspond to close to or the total saturation of resin volume. In general, REE recovery at the same concentration of the acids showed a trend of HNO_3 > HCl > H_2SO_4. In all three inorganic acids, the removal efficacy of the DMDODGA polymer was much stronger compared to the TODGA resin, particularly when using low concentrations of H_2SO_4 and HCl (0.01 and 0.1 M), rendering it a prospective EXC substrate for the hydrometallurgical recovery of REE [157].

EXC generally incorporates a number of the strengths of solvent extraction, primarily its specificity, with the ease and comfort of working with ion exchange materials. Applying the methods such as polymer microencapsulation may generate surfaces that are significantly more absorbent per unit of mass than any typical EXC sorbent, resulting in increased cation absorption capabilities [158]. The phase inversion precipitation and radiotracer process were used to create polysulfone microcapsules with sizes ranging from 50 to 100 µm that can be used in chromatographic extraction techniques using trivalent lanthanides. Solid–liquid (weight) distribution ratios (Dw) for the cations of relevance were evaluated radiometrically utilizing the ^{154}Eu radiotracer. The sorbents were used to quantify the absorption of ions from the HNO_3 medium by mixing a known amount (usually 1.0 mL) of a tracer-spiked acidic medium of optimum quantity with a fixed concentration of the sorbent [158].

In contrast to polysulfone macrocapsules, bis(2-ethylhexyl) phosphoric acid (HDEHP)-loaded microcapsules had a high ^{154}Eu partition ratio, with quick absorption kinetics and a high cation adsorption capacity. This capability far outperforms the commercially available extraction chromatographic matrix, due to the high extractant loadings attained with the microcapsules and the support-induced monomerization of HDEHP. These properties of the Ln-microcapsules, together with their cheap price and the simplicity of their production, indicated that they have potential value in the remediation of REEs, not only for analytical-scale recovery and purification for sequential evaluation, but similarly for process and preparative-scale usage [158].

In a comparative study, the chromatographic behavior of various cations was examined using a Celite column coated with Adogen-381 and a solvent mixture of KSCN or HCl. A variety of techniques for selectively isolating cations in one radiotracer form from one another was developed. The radiotracers utilized in this study were high in radiochemical purity: ^{60}Co, ^{65}Zn, ^{64}Cu, ^{115}Cd, ^{46}Sc, ^{141}Ce, ^{170}Tm, $^{152/154}$Eu, ^{59}Fe, ^{203}Hg, and ^{99}Mo (Table 1) [159].

Table 1. Isolation methods for various metal radiotracers [159] (Khalifa, S.M.; Raieh, M.; El-Dessouky, M.; Aly, H.F. Extraction chromatography of some metal radiotracers using adogen-381 HCl and KSCN systems. Chromatographia 1982, 15, 315–317, reproduced with permission of Springer Nature).

Metal Radiotracers Available			Eluted Radiotracer
Cu^{2+}, Fe^{3+}, Zn^{2+}, Hg^{2+}	3.75 cm^3	0.1M HCl	Fe^{3+}
	9.87 cm^3	4.0 KSCN	Cu^{2+}
	9.50 cm^3	8.0 M KSCN	Hg^{2+}
	2.50 cm^3	1.0 M H_4CH_3COO	Zn^{2+}
Sc^{3+}, Fe^{3+}, Hg^{2+}, Cd^{2+}	2.62 cm^3	8.0 M HCl	Sc^{3+}
	3.75 cm^3	0.1 M HCl	Fe^{3+}
	9.38 cm^3	8.0 M KSCN	Hg^{2+}
	3.75 cm^3	8.0 M HNO_3	Cd^{2+}
Co^{2+}, Cu^{2+}, Zn^{2+}	3.13 cm^3	4.0 M HCl	Co^{2+}
	9.37 cm^3	4.0 M KSCN	Cu^{2+}
	3.12 cm^3	1.0 M H_4CH_3COO	Zn^{2+}
Co^{2+}, Cu^{2+}, Cd^{2+}	5.62 cm^3	0.01 M HCl	Co^{2+}
	9.37 cm^3	4.0 M KSCN	Cu^{2+}
	3.75 cm^3	8.0 M HNO_3	Cd^{2+}
Cu^{2+}, Hg^{2+}, Cd^{2+}	9.50 cm^3	4.0 M KSCN	Cu^{2+}
	9.25 cm^3	8.0 M KSCN	$Hg2^+$
	7.75 cm^3	8.0 M HNO_3	Cd^{2+}
Sc^{3+}, Ce^{3+}, Eu^{3+}, Tm^{3+}, Cu^{2+}, Zn^{2+}	2.63 cm^3	0.1 M HCl	Sc^{3+}, Ce^{3+}, Eu^{3+}, Tm^{3+}
	9.63 cm^3	4.0 M KSCN	Cu^{2+}
	3.70 cm^3	1.0 M NH_4CH_3COO	Zn^{2+}
Sc^{3+}, Ce^{3+}, Eu^{3+}, Tm^{3+}, Mo^{6+}	2.25 cm^3	0.1 M HCl	Sc^{3+}, Ce^{3+}, Eu^{3+}, Tm^{3+}
	2.0 cm^3	4.0 M HNO_3	Mo^{6+}

The study observed that the chromatographic recovery methods for the cations can be established by employing their respective radiotracers to observe the cation's behavior in the chromatographic column of Table 1 [159]. It should be emphasized that after preconditioning with the loading solution, the column system can be utilized up to five times for every extraction without significantly changing the elution profile.

Likewise, the viability of separating Co and Sb from Zr in acid solutions can be conducted using the ion-exchange resins (Dowex 50-X8 and Dowex 1-X8 resins) [160]. Using ^{60}Co, ^{95}Zr, and ^{125}Sb radiotracers diluted in 0.25 mL HF and 0.25 mL HNO_3, the distribution coefficients of ^{60}Co, ^{95}Zr, and ^{125}Sb on potent cation and anion exchangers in HCl and oxalic acidic environments were evaluated [160]. Employing a High-Purity Germanium detector, the count rates of the solvents before and after equilibrium with the ion exchangers were monitored. The radioactivities of the tracers were calculated as count rates from the peak regions under the isotopes' characteristic gamma rays (^{60}Co, ^{95}Zr, and ^{125}Sb). The distribution coefficient K_D was computed as follows in Equation (14):

$$K_D = [A_0 - A] \times \frac{L}{m \times A} \tag{14}$$

wherein

- A_0 is the solution count rate prior to ion exchanger equilibration;
- A is the count rate of solvent following ion exchanger equilibration;
- L is the solution's volume (mL);
- m is the mass of ion exchange resin.

The K_Ds for both ^{95}Zr and ^{60}Co are high at lower HCl concentrations and reduce as the acidity increases. The reduction in ^{60}Co and ^{95}Zr distribution ratios with increasing

concentrations of HCl may be attributed to both the mass action of H^+ and the production of anionic matrixes at high HCl concentrations. It is feasible that, in low HCl concentrations, the $^{95}Zr^{4+}$ and $^{60}Co^{2+}$ present as cationic species and have enough exchange sites, leading to high K_D values. At a constant concentration of cation, the H^+ ions from HCl can compete with the metal ions of ^{60}Co and ^{95}Zr, leading to a drop in K_D values as the strength of the acid rises. For Sb, K_D ratios began to rise over 5 mol/L HCl [160]. It has recently been found that cations that are significantly absorbed by the anion exchanger from concentrated chloride solutions are likewise substantially absorbed by the cation exchanger. The degree of the distribution coefficient differs from the reported value because of variances in the degree of cross-linkage of the exchanger utilized and/or the incredibly minimal concentration of Sb [160]. The above findings indicate the importance of nuclear chemistry in the study and development of chromatographic surfaces for the separation and recovery of the various cations.

Because of their favorable nuclear properties, such as energy and half-life, and chemical properties, such as ease of complexation with a range of organic compounds, In radioisotopes are employed for diagnostics [161,162]. The carrier-free indium radioisotopes ^{115m}In and ^{111}In are commonly utilized. On a chromatographic column loaded with TODGA-impregnated silica gel, a radiotracer method was employed to attain carrier-free isolation of ^{115m}In from its parent ^{115}Cd in an HCl medium [161]. Both cations bound at the chelating site at 8 M HCl, resulting in maximal adsorption. When the column was treated with 2 M HCl, the daughter complex was desorbed and released from the column, while the parent complex was left uninterrupted. Under these conditions, pure silica gel did not absorb radioactivity. The daughter's radiochemical purity was evaluated using its half-life of 4.49 hrs [161].

Likewise, a chromatographic column filled with TODGA-impregnated silica gel can be applied in separating trace concentrations of Ag^+ from the HNO_3 media utilizing a ^{110m}Ag radiotracer [163]. Ag has been highly consumed in society due to its valued characteristics. As a result, it is critical to create a sensitive and specific approach for determining and separating Ag. At various temperatures and acid concentrations, the adsorption of Ag on such a column was investigated [163]. The highest adsorption was seen at 10^{-7} M of HNO_3 acid, using the ^{110m}Ag radiotracer at neutral pH to analyze the Ag^+ adsorption in relation to the concentration of HNO_3.

However, while studying the kinetics of the processes, at 30 °C, the adsorption of $^{110m}Ag^+$ on TODGA-impregnated silica gel was investigated at adsorptive concentrations ranging from $(4–60) \times 10^{-4}$ M. The uptake of $^{110m}Ag^+$ ions was initially rapid, but it slowed over time, and saturation was established within 10 min. Even after 6 h of interaction, no further $^{110m}Ag^+$ uptake was seen. However, when the solution concentration was reduced from 6×10^{-4} to 4×10^{-4} M, the percentage of $^{110m}Ag^+$ absorption increased from 52.4 to 98.1%. The restricted number of active sites available for $^{110m}Ag^+$ sorption could explain this rise in $^{110m}Ag^+$ uptake % [163]. Radiotracer techniques are, therefore, crucial in the study of the various processes involved in hydrometallurgy [111].

4. Product Analyses

The recovered metals from leaching, solvent extraction, adsorption, and from chromatographic resins can be quantified using INAA. The recovered metals in solution or solid form can be irradiated by neutrons with the appropriate neutron flux. Thereafter, the quantification process is conducted by measuring the gamma spectrum over some time. The resulting gamma-ray spectrum is then interpreted and the type and quantity of a given element are determined. An important aspect is to find the relationship between the concentration and activity of a given radionuclide. It can be represented by the Formula (15) [164]

$$A_0 = N \cdot \phi \cdot \sigma \cdot \left(1 - e^{-\lambda \cdot t}\right) \tag{15}$$

where;

- A$_0$ is the activity of the excited radionuclide excited due to irradiation of the sample with neutrons; activity is expressed in [Bq], which is the number of decays per second;
- N is the atomic number of a given isotope in the target material;
- ϕ is the neutron flux density (cm^{-2}s^{-1});
- σ is the activation cross-section, which is the probability of a nuclear reaction occurring expressed in cm^2; 1 barn $= 10^{-24}$ cm^2);
- t is the irradiation time [s];
- λ is the radioactive decay constant: $\lambda = \frac{\ln 2}{T}$;
- T is the half-life of the radionuclide [s];
- $\left(1 - e^{-\lambda \cdot t}\right)$ is the saturation factor, representing the fraction of the maximum obtainable activity after irradiation.

In practice, activity is not measured directly; however, the amount of the analyte is proportional to the number of counts. The easiest and most accurate way to calculate the mass of the analyzed element is the method of the standard, which is irradiated together with the tested samples. The formula for calculating the concentration of the metal of interest is presented in the following form [107]:

$$x = \frac{\left(\frac{P}{D \cdot C \cdot m_P}\right)_{\text{samples}}}{\left(\frac{P}{D \cdot C \cdot m_w}\right)_{\text{pattern}}} \tag{16}$$

where;

- x is the concentration of the determined element (ppm);
- P is the number of counts collected in a given peak;
- D is the correction for nuclide decay before starting the measurements;
- C is the factor responsible for the decay of the radionuclide during the measurements;
- m$_p$ is the sample weight [g];
- m$_w$ is the mass of the standard [μg].

The relationship expressed by Equation (16) allows the calculation of the metal concentration during research on an active sample.

The product can also be analyzed using the XRF technique. XRF can evaluate nearly every single substance placed in the spectrometer, but the better the sample preparation, the more precise and reliable the analytical outcome. The sample preparation method will always be a trade-off between the quality of outcomes required, the effort applied in due course (i.e., labor and complexity), and the expenses (i.e., sample preparation equipment and time to analysis labor) [165]. Based on the analysis requirements, the choice might vary for different components. Pellets can be generated for the proper geometry necessary for the efficient interaction of the X-rays with the components of the sample [166]. When analyzing a loose powdered substance, the specimen can be placed in a plastic sample cup with a plastic support film. That ensures a flat surface for the X-ray analyzer and supports the specimen over the X-ray beam. The finer the material, the more likely it is to be homogeneous and have reduced empty spaces, allowing for a more accurate analysis. Enough powder should be used to achieve an infinite surface area for all of the metals of concern.

As with loose powdered samples, liquid samples are prepared by transferring them into a plastic sample cup. There are few possibilities for analyzing liquid samples, and the important factor is to select the proper support film that offers a balance of transmission capabilities, strength, and contamination. Mylar is an ideal film, but polypropylene improves transmission more than mylar, although it has a lower tensile strength. Kapton is an excellent film, but it dramatically represses the XRF signal for lighter elements and is vulnerable to highly basic solutions [165]. For reliable results, the appropriate film for liquid samples must be chosen. In general, different software integrated into the XRF can provide the concentrations of the elements present in the sample under analysis (solid). In

addition to XRF and NAA, XRD, XANES, EXAFS, XPS, and XAS can be used to characterize the recovered metals. Such techniques give information regarding the structural orientation and surface analysis of the recovered metals.

5. Conclusions

Since industrialization, there has been a significant rise in the utilization of energy reserves, especially fossil fuels. The available critical and strategic metals have declined dramatically due to intensive mining and urbanization, among other things. Hydrometallurgical procedures must be developed to increase the recovery of key metals. Isotope tracers for studying the physicochemical foundations of processes, laboratory industrial technology studies, and a method for researching the effectiveness of existing industrial technologies and apparatus, as well as the control and regulation of industrial processes, are all beneficial in the study of hydrometallurgical issues. Using radiotracers in solvent extraction, adsorption and chromatographic resins enhance the study of the behavior of cations recovery. Radiometric analysis, such as the neutron activation methods, and X-Ray Fluorescence are important in the analysis of the metals. The employment of nuclear technology to control and regulate technical processes has aided numerous industries in optimizing industrial operations and finding flaws. The described applications of radiotracers, methodologies, and analyses can be used directly to optimize hydrometallurgical processes and installations on laboratory and industrial scales.

References

1. Tausova, M.; Culkova, K.; Domaracká, L.; Drebenstedt, C.; Taušová, M.; Čulková, K.; Muchová, M.S.; Koščo, J.; Behúnová, A.; Drevková, M.; et al. The importance of mining for socio-economic growth of the country. *Acta Montan. Slovaca* **2017**, *22*, 359–367.
2. Ascher, W. *Why Governments Waste Natural Resources: Policy Failures in Developing Countries*; JHU Press: Baltimore, MD, USA, 1999.
3. Wojciech, K. *MINLEX -Poland Country Report*; MinPol and partner: Warsaw, Poland, 2019; pp. 1–95. Available online: https://rmis.jrc.ec.europa.eu/uploads/legislation/MINLEX_CountryReport_PL.pdf (accessed on 17 October 2022).
4. Maina, D.M.; Ndirangu, D.M.; Mangala, M.M.; Boman, J.; Shepherd, K.; Gatari, M.J. Environmental implications of high metal content in soils of a titanium mining zone in Kenya. *Environ. Sci. Pollut. Res.* **2016**, *23*, 21431–21440. [CrossRef] [PubMed]
5. Ceniceros-Gómez, A.E.; Macías-Macías, K.Y.; de la Cruz-Moreno, J.E.; Gutiérrez-Ruiz, M.E.; Martínez-Jardines, L.G. Characterization of mining tailings in México for the possible recovery of strategic elements. *J. South Am. Earth Sci.* **2018**, *88*, 72–79. [CrossRef]
6. Kirsten, H.; Daniele, L.P.; Thao, F.; Tim, L.; John, D. *Minerals for Climate Action: The Mineral Intensity of the Clean Energy Transition*; The World Bank: Washington, WA, USA, 2020; pp. 1–112. Available online: https://pubdocs.worldbank.org/en/961711588875536384/Minerals-for-Climate-Action-The-Mineral-Intensity-of-the-Clean-Energy-Transition.pdf (accessed on 27 January 2023).
7. Kim, J.; Guillaume, B.; Chung, J.; Hwang, Y. Critical and precious materials consumption and requirement in wind energy system in the EU 27. *Appl. Energy* **2015**, *139*, 327–334. [CrossRef]
8. Grandell, L.; Lehtilä, A.; Kivinen, M.; Koljonen, T.; Kihlman, S.; Lauri, L.S. Role of critical metals in the future markets of clean energy technologies. *Renew. Energy* **2016**, *95*, 53–62. [CrossRef]
9. Moss, R.L.; Tzimas, E.; Kara, H.; Willis, P.; Kooroshy, J. Critical Metals in Strategic Energy Technologies: Assessing rare metals as supply-chain bottlenecks in low-carbon energy technologies. In *JRC-scientific and strategic reports, European Commission Joint Research Centre Institute for Energy and Transport*; Institute for Energy and Transport IET: Hague,The Netherlands, 2011. [CrossRef]

10. Zhang, S.; Ding, Y.; Liu, B.; Chang, C.C. Supply and demand of some critical metals and present status of their recycling in WEEE. *Waste Manag.* **2017**, *65*, 113–127. [CrossRef]

11. Habib, K.; Hansdóttir, S.T.; Habib, H. Critical metals for electromobility: Global demand scenarios for passenger vehicles, 2015–2050. *Resour. Conserv. Recycl.* **2020**, *154*, 104603. [CrossRef]

12. Blengini, G.A.; Mathieux, F.; Mancini, L.; Nyberg, M.; Cavaco Viegas, H.; Salminen, J.; Garbarino, E.; Orveillion, G.; Saveyn, H. Recovery of critical and other raw materials from mining waste and landfills. In *JRC Science for Policy Report*; European Commission: Maastricht, The Netherlands, 2019. [CrossRef]

13. Ayres, R.U.; Peiró, L.T. Material efficiency: Rare and critical metals. *Philos. Trans. R. Soc. A Math. Phys. Eng. Sci.* **2013**, *371*, 20110563. [CrossRef]

14. Žibret, G.; Lemiere, B.; Mendez, A.M.; Cormio, C.; Sinnett, D.; Cleall, P.; Szabo, K.; Carvalho, T. National mineral waste databases as an information source for assessing material recovery potential from mine waste, tailings and metallurgical waste. *Minerals* **2020**, *10*, 446. [CrossRef]

15. Purwadi, I.; van der Werff, H.M.A.; Lievens, C. Targeting rare earth element bearing mine tailings on Bangka Island, Indonesia, with Sentinel-2 MSI. *Int. J. Appl. Earth Obs. Geoinf.* **2020**, *88*, 102055. [CrossRef]

16. Wang, L.; Liang, T. Geochemical fractions of rare earth elements in soil around a mine tailing in Baotou, China. *Sci. Rep.* **2015**, *5*, 1–11. [CrossRef] [PubMed]

17. Campbell, G.A. Rare earth metals: A strategic concern. *Miner. Econ.* **2014**, *27*, 21–31. [CrossRef]

18. Zhuang, W.Q.; Fitts, J.P.; Ajo-Franklin, C.M.; Maes, S.; Alvarez-Cohen, L.; Hennebel, T. Recovery of critical metals using biometallurgy. *Curr. Opin. Biotechnol.* **2015**, *33*, 327–335. [CrossRef] [PubMed]

19. Deblonde, G.J.P.; Chagnes, A.; Cote, G. Recent Advances in the chemistry of hydrometallurgical methods. *Sep. Purif. Rev.* **2022**, 1. [CrossRef]

20. Seetharaman, S.; McLean, A.; Guthrie, R.; Sridhar, S. *Treatise on Process Metallurgy, Volume 3: Industrial processes*; Newnes: Tokyo, Japan, 2013; Volume 3.

21. Galos, K.; Kot-Niewiadomska, A.; Kamyk, J. The Role of Poland in the European Union Supply Chain of Raw Materials, Including Critical Raw Materials. *Mater. Proc.* **2021**, *5*, 14. [CrossRef]

22. Fleming, P.; Orrego, P.; Pinilla, F. Recovery of Rare Earth Elements Present in Mining Tails, by Leaching with Nitric and Hydrochloric Solutions. *World J. Nucl. Sci. Technol.* **2021**, *11*, 1–16. [CrossRef]

23. Chakhmouradian, A.R.; Smith, M.P.; Kynicky, J. From "strategic" tungsten to "green" neodymium: A century of critical metals at a glance. *Ore Geol. Rev.* **2015**, *64*, 455–458. [CrossRef]

24. House of Commons. *House of Commons Science and Technology Committee: HC 726; Strategically Important Metals; Fifth Report of Session 2010-12*; 2011. Available online: www.parliament.uk/science (accessed on 20 October 2022).

25. Martin, G.; Rentsch, L.; Höck, M.; Bertau, M. Lithium market research—global supply, future demand and price development. *Energy Storage Mater.* **2017**, *6*, 171–179. [CrossRef]

26. Field, F.R.; Wallington, T.J.; Everson, M.; Kirchain, R.E. Strategic Materials in the Automobile: A Comprehensive Assessment of Strategic and Minor Metals Use in Passenger Cars and Light Trucks. *Environ. Sci. Technol.* **2017**, *51*, 14436–14444. [CrossRef]

27. Zuo, L.; Wang, C.; Corder, G.D. Strategic evaluation of recycling high-tech metals from urban mines in China: An emerging industrial perspective. *J. Clean. Prod.* **2019**, *208*, 697–708. [CrossRef]

28. Mishra, B.; Anderson, C.D.; Taylor, P.R.; Anderson, C.G.; Apelian, D.; Blanpain, B. CR3 update: Recycling of strategic metals. *Jom* **2012**, *64*, 441–443. [CrossRef]

29. Calvo, G.; Valero, A.; Valero, A. How can strategic metals drive the economy? Tungsten and tin production in Spain during periods of war. *Extr. Ind. Soc.* **2019**, *6*, 8–14. [CrossRef]

30. Jha, M.K.; Kumari, A.; Panda, R.; Rajesh Kumar, J.; Yoo, K.; Lee, J.Y. Review on hydrometallurgical recovery of rare earth metals. *Hydrometallurgy* **2016**, *165*, 2–26. [CrossRef]

31. Iannicelli-Zubiani, E.M.; Giani, M.I.; Recanati, F.; Dotelli, G.; Puricelli, S.; Cristiani, C. Environmental impacts of a hydromet-allurgical process for electronic waste treatment: A life cycle assessment case study. *J. Clean. Prod.* **2017**, *140*, 1204–1216. [CrossRef]

32. International Atomic Energy Agency. The Current Status and Future Trends on Radioisotope Applications in Industry. *Expert Rev. Med. Devices* **2012**, *7*, 331–343.

33. Pant, H.J. Applications of the radiotracers in the industry: A review. *Appl. Radiat. Isot.* **2022**, *182*, 110076. [CrossRef]

34. Teviso Sensor Technologies Ltd. 2023. Available online: https://www.teviso.com/ (accessed on 27 January 2023).

35. Company | TD-Electronics. 2023. Available online: https://td-electronics.pl/en/company/ (accessed on 27 January 2023).

36. CSIRO. *Commonwealth Scientific and Industrial Research Organisation, Australian Government*; CSIRO: Canberra, Australia, 2023.

37. Li, M.; Deng, R.; Cao, J.; Qiu, J.; Lei, G.; Li, X.; Zhang, B. Research on remaining oil evaluation method based on cased hole logging technology. *Energy Rep.* **2021**, *7*, 1168–1174. [CrossRef]

38. Fan, J.; Zhang, F.; Tian, L.; Liang, Q.; Zhang, X.; Fang, Q.; Lu, B.; Li, X. A method of monitoring gas saturation in carbon dioxide injection heavy oil reservoirs by pulsed neutron logging technology. *Pet. Explor. Dev.* **2021**, *48*, 1420–1429. [CrossRef]

39. Pant, H.J.; Kundu, A.; Nigam, K.D.P. Radiotracer applications in chemical process industry. *Rev. Chem. Eng.* **2001**, *17*, 165–252. [CrossRef]

40. Vanhoof, C.; Bacon, J.R.; Fittschen, U.E.A.; Vincze, L. Atomic spectrometry update—A review of advances in X-ray fluorescence spectrometry and its special applications. *J. Anal. At. Spectrom.* **2021**, *36*, 1797–1812. [CrossRef]

41. Zhang, Y.; He, Y.; Zhou, W.; Mo, G.; Chen, H.; Xu, T. Review on the elemental analysis of polymetallic deposits by total-reflection X-ray fluorescence spectrometry. *Appl. Spectrosc. Rev.* **2022**, 1–14. [CrossRef]

42. Khan, H.; Yerramilli, A.S.; D'Oliveira, A.; Alford, T.L.; Boffito, D.C.; Patience, G.S. Experimental methods in chemical engineering: X-ray diffraction spectroscopy—XRD. *Can. J. Chem. Eng.* **2020**, *98*, 1255–1266. [CrossRef]

43. Ali, A.; Chiang, Y.W.; Santos, R.M. X-Ray Diffraction Techniques for Mineral Characterization: A Review for Engineers of the Fundamentals, Applications, and Research Directions. *Minerals* **2022**, *12*, 205. [CrossRef]

44. Feng, X.; Onel, O.; Council-Troche, M.; Noble, A.; Yoon, R.H.; Morris, J.R. A study of rare earth ion-adsorption clays: The speciation of rare earth elements on kaolinite at basic pH. *Appl. Clay Sci.* **2021**, *201*, 105920. [CrossRef]

45. Habashi, F. A short history of hydrometallurgy. *Hydrometallurgy* **2005**, *79*, 15–22. [CrossRef]

46. Botelho Junior, A.B.; Dreisinger, D.B.; Espinosa, D.C.R. A Review of Nickel, Copper, and Cobalt Recovery by Chelating Ion Exchange Resins from Mining Processes and Mining Tailings. *Min. Metall. Explor.* **2019**, *36*, 199–213. [CrossRef]

47. Florek, J.; Giret, S.; Juère, E.; Larivière, D.; Kleitz, F. Functionalization of mesoporous materials for lanthanide and actinide extraction. *Dalton Trans.* **2016**, *45*, 14832. [CrossRef]

48. Um, N.; Um, N. Hydrometallurgical Recovery Process of Rare Earth Elements from Waste: Main Application of Acid Leaching with Devised τ-T Diagram. *Rare Earth Elem.* **2017**, 44–58. [CrossRef]

49. Zeng, L.; Cheng, C.Y. A literature review of the recovery of molybdenum and vanadium from spent hydrodesulphurisation catalysts: Part I: Metallurgical processes. *Hydrometallurgy* **2009**, *98*, 1–9. [CrossRef]

50. Sun, H.; Liu, Y.; Lin, J.; Yue, Z.; Li, W.; Jin, J.; Sun, Q.; Ai, Y.; Feng, M.; Huang, X. Highly Selective Recovery of Lanthanides by Using a Layered Vanadate with Acid and Radiation Resistance. *Angew. Chem.* **2020**, *132*, 1894–1899. [CrossRef]

51. Rogowski, M.; Smolinski, T.; Pyszynska, M.; Brykala, M.; Chmielewski, A.G. Studies on hydrometallurgical processes using nuclear techniques to be applied in copper industry. II. Application of radiotracers in copper leaching from flotation tailings. *Nukleonika* **2018**, *63*, 131–137. [CrossRef]

52. Sharma, S.; Tiwari, S.; Hasan, A.; Saxena, V.; Pandey, L.M. Recent advances in conventional and contemporary methods for remediation of heavy metal-contaminated soils. *3 Biotech* **2018**, *8*, 4. [CrossRef] [PubMed]

53. Narbutt, J.; Chmielewski, A.G. Stan Obecny Oraz Perspektywy Rozwoju Radiochemii i Chemii Jądrowej w Polsce. 2001. Available online: https://scholar.google.com/scholar?hl=en&as_sdt=0%2C5&q=Jerzy+Narbutt%2C+Andrzej+G.+Chmielewski%2C+STAN+OBECNYORAZ+PERSPEKTYWY+ROZWOJU+RADIOCHEMII+I+CHEMII+J\relax$A$DROWEJ+W++POLSCE%2C+RAPORTY+IChTJ.+SERIA+B+nr+1%2F2001&btnG= (accessed on 13 April 2022).

54. Dybczyński, R.S. The role of NAA in securing the accuracy of analytical results in the inorganic trace analysis. *J. Radioanal. Nucl. Chem.* **2019**, *322*, 1505–1515. [CrossRef]

55. Yao, M.; Wang, D.; Zhao, M. Element Analysis Based on Energy-Dispersive X-Ray Fluorescence. *Adv. Mater. Sci. Eng.* **2015**, *2015*, 290593. [CrossRef]

56. Regadío, M.; Riaň, S.; Binnemans, K.; Hoogerstraete, T.V. Direct Analysis of Metal Ions in Solutions with High Salt Concentrations by Total Reflection X-ray Fluorescence. *Anal. Chem.* **2017**, *89*, 4595–4603. [CrossRef]

57. Omran, E.; Abd, A.A.; Razek, E. Mapping and screening risk assessment of heavy metals concentrations in soils of the Bahr El-Baker Region, Egypt. *Undefined* **2012**, *3*, 182–195. [CrossRef]

58. Przewlocki, K.; Petryka, L.; Stegowski, Z. Radiotracer Investigation of the Copper Ore Concentration Process. In *Isotopenpraxis Isotopes in Environmental and Health Studies*; Taylor & Francis Group: Abingdon, UK, 1990; pp. 439–444. [CrossRef]

59. Nkuna, R.; Ijoma, G.N.; Matambo, T.S.; Chimwani, N. Accessing Metals from Low-Grade Ores and the Environmental Impact Considerations: A Review of the Perspectives of Conventional versus Bioleaching Strategies. *Minerals* **2022**, *12*, 506. [CrossRef]

60. Nad, A.; Jooshaki, M.; Tuominen, E.; Michaux, S.; Kirpala, A.; Newcomb, J. Digitalization Solutions in the Mineral Processing Industry: The Case of GTK Mintec, Finland. *Minerals* **2022**, *12*, 210. [CrossRef]

61. International Atomic Energy Agency. *TECHNOLOGY TRANSFER OF NUCLEAR TECHNIQUES AND NUCLEONIC CONTROL SYSTEMS IN THE MINERAL INDUSTRY.* 1990. Available online: https://www-pub.iaea.org/MTCD/Publications/PDF/te_0578.pdf (accessed on 18 October 2022).

62. Brisset, P.; Miskovic, S. Development of Radiometric Methods for Exploration and Process Optimization in Mining and Mineral Industries. *IAEA Vienna Sept.* 2014, pp. 1–5. Available online: http://www-naweb.iaea.org/napc/iachem/working_materials/CM7%20Meeting%20on%20preparation%20of%20a%20CRP%20in%20Mining%20industry%20-%20Report%20-%20Final.pdf (accessed on 18 October 2022).

63. Kraś, J.; Nobis, C.; Myczkowski, S. Leakage Control Methods for Metal Underground Tanks and Tanks Placed on Hardened Soil with the Use of Radioactive Tracers. *Nukleonika* **2008**, *2*, 137–140. Available online: https://www.infona.pl/resource/bwmeta1.element.baztech-3162594f-579f-439a-934c-eb34be8a80a0 (accessed on 24 October 2022).

64. Petryka, L.; Przewlocki, K. Optimization of Copper Ore Concentration Processing by Means of Radioactive Tracers. *Isot. Isot. Environ. Health Stud.* **1989**, *25*, 139–143. [CrossRef]

65. Thereska, J.; Çuçi, T.; Plasari, E.; Lleshi, Z. Radiotracer determination of gold recovery in copper melting process. *J. Radioanal. Nucl. Chem. Lett.* **1989**, *136*, 197–202. [CrossRef]

66. Michalik, J.S.; Palige, J.; Bazaniak, Z. Radiotracer Investigations of the Shaft Processes in Polish Zine and Lead Metallurgy Part. I. Investigation of Charge Materials Movement. *Isot. Isot. Environ. Health Stud.* **1990**, *26*, 210–215. [CrossRef]

67. Bazaniak, Z.; Klimkiewicz, T. *Studies on Reduction Process of Cu2O in an Electric Furnace Using Radiotracers*; Taylor & Francis: Abingdon, UK, 1983; Volume 19, pp. 373–376. [CrossRef]

68. Rosenberg, R.J.; Guizerix, J. Nuclear techniques for peaceful development Nuclear techniques in mineral exploration, extraction, and processing Overview of typical applications and the IAEA's activities in the field. *IAEA Bull.* **1987**, *29*, 28–32.

69. Glascock, M.D. *An Overview of Neutron Activation Analysis*; University of Missouri Research Reactor (MURR): Columbia, MO, USA, 2006.

70. El-Taher, A.; Kratz, K.L.; Nossair, A.; Azzam, A.H. Determination of gold in two Egyptian gold ores using instrumental neutron activation analysis. *Radiat. Phys. Chem.* **2003**, *68*, 751–755. [CrossRef]

71. El-Taher, A. Elemental analysis of two Egyptian phosphate rock mines by instrumental neutron activation analysis and atomic absorption spectrometry. *Appl. Radiat. Isot.* **2010**, *68*, 511–515. [CrossRef]

72. Nandy, M.; Nandy, M. Neutron Activation Analysis: Application in Geology and Medicine. In *Advanced Technologies and Applications of Neutron Activation Analysis*; IntechOpen: London, UK, 2019. [CrossRef]

73. Zovko, E.; Islamović, S. Application of neutron activation in hydrometallurgical process of lead chloride extraction from boulangerit. *Hem. Ind.* **2010**, *64*, 53–55. [CrossRef]

74. Smolik, M.; Polkowska-Motrenko, H.; Hubicki, Z.; Jakóbik-Kolon, A.; Danko, B. Determination of hafnium at the 10-4% level (relative to zirconium content) using neutron activation analysis, inductively coupled plasma mass spectrometry and inductively coupled plasma atomic emission spectrometry. *Anal. Chim. Acta* **2014**, *806*, 97–100. [CrossRef]

75. Osawa, T.; Hatsukawa, Y.; Appel, P.W.U.; Matsue, H. Mercury and gold concentrations of highly polluted environmental samples determined using prompt gamma-ray analysis and instrument neutron activation analysis. *Nucl. Instrum. Methods Phys. Res. Sect. B Beam Interact. Mater. At.* **2011**, *269*, 717–720. [CrossRef]

76. Rotich, N.K. Evaluation of the Essential Trace Metals in Soils and African Spider Plants: Case Study of Molo Ward-Nakuru County [University of Nairobi]. 2019. Available online: http://erepository.uonbi.ac.ke/handle/11295/108854 (accessed on 31 October 2022).

77. Brouwer, P. *Theory of X-ray Fluorescence. Getting Acquainted with the Principles*, 3rd ed.; PANalytical, B.V., Ed.; PANanalytical: Malvern, UK, 2013.

78. Goldstein, J.I.; Newbury, D.E.; Echlin, P.; Joy, D.C.; Lyman, C.E.; Lifshin, E.; Sawyer, L.; Michael, J.R. *Scanning Electron Microscopy and X-ray Microanalysis and analytical ELECTRON Microscopy*; Springer: Berlin/Heidelberg, Germany, 2003. [CrossRef]

79. Kuhn, K.; Meima, J.A.; Rammlmair, D.; Ohlendorf, C. Chemical mapping of mine waste drill cores with laser-induced breakdown spectroscopy (LIBS) and energy dispersive X-ray fluorescence (EDXRF) for mineral resource exploration. *J. Geochem. Explor.* **2015**, *161*, 72–84. [CrossRef]

80. Gonzalez-Fernandez, O.; Queralt, I.; Carvalho, M.L.; Garcia, G. Elemental analysis of mining wastes by energy dispersive X-ray fluorescence (EDXRF). *Nucl. Instrum. Methods Phys. Res. Sect. B Beam Interact. Mater. At.* **2007**, *262*, 81–86. [CrossRef]

81. Gonzalez-Fernandez, O.; Queralt, I. Fast elemental screening of soil and sediment profiles using small-spot energy-dispersive X-ray fluorescence: Application to mining sediments geochemistry. *Appl. Spectrosc.* **2010**, *64*, 1045–1053. [CrossRef]

82. Remya Devi, P.S.; Trupti, A.C.; Nicy, A.; Dalvi, A.A.; Swain, K.K.; Wagh, D.N.; Verma, R. Evaluation of uncertainty in the energy dispersive X-ray fluorescence determination of platinum in alumina. *Anal. Methods* **2015**, *7*, 5345–5351. [CrossRef]

83. Craddock, P.R.; Herron, M.M.; Herron, S.L. COMPARISON OF QUANTITATIVE MINERAL ANALYSIS BY X-RAY DIFFRACTION AND FOURIER TRANSFORM INFRARED SPECTROSCOPY. *J. Sediment. Res.* **2017**, *87*, 630–652. [CrossRef]

84. Majuste, D.; Ciminelli, V.S.T.; Eng, P.J.; Osseo-Asare, K. Applications of in situ synchrotron XRD in hydrometallurgy: Literature review and investigation of chalcopyrite dissolution. *Hydrometallurgy* **2013**, *131–132*, 54–66. [CrossRef]

85. Stevie, F.A.; Donley, C.L. Introduction to x-ray photoelectron spectroscopy. *J. Vac. Sci. Technol. A Vac. Surf. Film.* **2020**, *38*, 063204. [CrossRef]

86. Yano, J.; Yachandra, V.K. X-ray absorption spectroscopy. *Photosynth. Res.* **2009**, *102*, 241–254. [CrossRef] [PubMed]

87. Baba, A.A.; Adekola, F.A. Hydrometallurgical processing of a Nigerian sphalerite in hydrochloric acid: Characterization and dissolution kinetics. *Hydrometallurgy* **2010**, *101*, 69–75. [CrossRef]

88. Majuste, D.; Ciminelli, V.S.T.; Osseo-Asare, K.; Dantas, M.S.S.; Magalhães-Paniago, R. Electrochemical dissolution of chalcopyrite: Detection of bornite by synchrotron small angle X-ray diffraction and its correlation with the hindered dissolution process. *Hydrometallurgy* **2012**, *111–112*, 114–123. [CrossRef]

89. Xia, J.L.; Song, J.J.; Liu, H.C.; Nie, Z.Y.; Shen, L.; Yuan, P.; Ma, C.Y.; Zheng, L.; Zhao, Y.D. Study on catalytic mechanism of silver ions in bioleaching of chalcopyrite by SR-XRD and XANES. *Hydrometallurgy* **2018**, *180*, 26–35. [CrossRef]

90. Watari, T.; Nansai, K.; Nakajima, K. Review of critical metal dynamics to 2050 for 48 elements. *Resour. Conserv. Recycl.* **2020**, *155*, 104669. [CrossRef]

91. Kim, W.J.; Seo, S.; Lee, S.I.; Kim, D.W.; Kim, M.J. A study on pyro-hydrometallurgical process for selective recovery of Pb, Sn and Sb from lead dross. *J. Hazard. Mater.* **2021**, *417*, 126071. [CrossRef]

92. Rabatho, J.P.; Tongamp, W.; Takasaki, Y.; Haga, K.; Shibayama, A. Recovery of Nd and Dy from rare earth magnetic waste sludge by hydrometallurgical process. *J. Mater. Cycles Waste Manag.* **2012**, *15*, 171–178. [CrossRef]

93. Han, H.; Sun, W.; Hu, Y.; Cao, X.; Tang, H.; Liu, R.; Yue, T. Magnetite precipitation for iron removal from nickel-rich solutions in hydrometallurgy process. *Hydrometallurgy* **2016**, *165*, 318–322. [CrossRef]

94. Pathak, N.; Sen, R. Analytical Application of Radioactive Analysis. *Int. J. Anal. Appl. Chem.* **2017**, *3*, 32–35. Available online: https://chemical.journalspub.info/index.php?journal=JAAC&page=article&op=view&path%5B%5D=410 (accessed on 18 October 2022).

95. Gitau, J.; Gatari, M.J.; Pant, H.J. Investigation of flow dynamics of porous clinkers in a ball mill using technitium-99m as a radiotracer. *Appl. Radiat. Isot.* **2019**, *154*, 108902. [CrossRef]

96. Othman, N.; Kamarudin, S.K. Radiotracer technology in mixing processes for industrial applications. *Sci. World J.* **2014**, *2014*, 768604. [CrossRef] [PubMed]

97. Sheoran, M.; Chandra, A.; Bhunia, H.; Bajpai, P.K.; Pant, H.J. Residence time distribution studies using radiotracers in chemical industry—A review. *Chem. Eng. Commun.* **2018**, *205*, 739–758. [CrossRef]

98. el Korchi, K.; Alami, R.; Saadaoui, A.; Mimount, S.; Chaouch, A. Residence time distribution studies using radiotracers in a lab-scale distillation column: Experiments and modeling. *Appl. Radiat. Isot.* **2019**, *154*, 108889. [CrossRef]

99. Din, G.U.; Khan, I.H.; Chughtai, I.R.; Inayat, M.H.; Jin, J.H. Radiotracer investigations to study the hydrodynamic characteristics of continuous phase in a pulsed sieve plate extraction column. *EPJ Web Conf.* **2013**, *50*, 01004. [CrossRef]

100. Pant, H.J.; Sharma, V.K.; Naik, S.V.; Singh, G.; Kalgutkar, D.B.; Patil, S.P.; Jayachandran, N.; Unni, V.K.P. Investigation of leaching of an antifouling agent from marine paint formulations using radiotracer technique. *J. Radioanal. Nucl. Chem.* **2012**, *294*, 65–69. [CrossRef]

101. Goswami, S.; Biswal, J.; Samantray, J.; Gupta, D.F.; Pant, H.J. Measurement of mixing time and holdup of solids in gas–solid fluidized bed using radiotracer technique. *J. Radioanal. Nucl. Chem.* **2014**, *302*, 845–850. [CrossRef]

102. Kasban, H.; Arafa, H.; Elaraby, S.M.S. Principle component analysis for radiotracer signal separation. *Appl. Radiat. Isot.* **2016**, *112*, 20–26. [CrossRef] [PubMed]

103. Pant, H.J.; Sharma, V.K.; Singh, G.; Raman, V.K.; Bornare, J.; Sonde, R.R. Radiotracer investigation in a rotary fluidized bioreactor. *J. Radioanal. Nucl. Chem.* **2012**, *294*, 59–63. [CrossRef]

104. Pant, H.J.; Sharma, V.K.; Shenoy, K.T.; Sreenivas, T. Measurements of liquid phase residence time distributions in a pilot-scale continuous leaching reactor using radiotracer technique. *Appl. Radiat. Isot.* **2015**, *97*, 40–46. [CrossRef]

105. Domínguez, J.; Abreu, A.M.; McCalla, R.; Borroto, J.; Ortueta, M.; Pérez, E. Mixing characterization in batch reactors using the radiotracer technique. *J. Radioanal. Nucl. Chem.* **1999**, *241*, 337–340. [CrossRef]

106. Kaya, M. Current WEEE recycling solutions. In *Waste Electrical and Electronic Equipment Recycling: Aqueous Recovery Methods*; Woodhead Publishing: Sawston, UK, 2018; pp. 33–93. [CrossRef]

107. Smolinski, T.; Rogowski, M.; Brykala, M.; Pyszynska, M.; Chmielewski, A.G. Studies on hydrometallurgical processes using nuclear techniques to be applied in copper industry. I. Application of 64Cu radiotracer for investigation of copper ore leaching. *Nukleonika* **2018**, *63*, 123–129. [CrossRef]

108. Alvial-Hein, G.; Mahandra, H.; Ghahreman, A. Separation and recovery of cobalt and nickel from end of life products via solvent extraction technique: A review. *J. Clean. Prod.* **2021**, *297*, 126592. [CrossRef]

109. Panigrahi, M.; Grabda, M.; Kozak, D.; Dorai, A.; Shibata, E.; Kawamura, J.; Nakamura, T. Liquid–liquid extraction of neodymium ions from aqueous solutions of NdCl3 by phosphonium-based ionic liquids. *Sep. Purif. Technol.* **2016**, *171*, 263–269. [CrossRef]

110. Li, Z.; Zhang, Z.; Smolders, S.; Li, X.; Raiguel, S.; Nies, E.; de Vos, D.E.; Binnemans, K. Enhancing Metal Separations by Liquid–Liquid Extraction Using Polar Solvents. *Chem. -A Eur. J.* **2019**, *25*, 9197–9201. [CrossRef]

111. Gloe, K.; Mühl, P. Determination of Metal Extraction Process Parameters Using Tracer Technique. *Isot. Isot. Environ. Health Stud.* **1983**, *19*, 257–260. [CrossRef]

112. Sarkar, R.; Dey, P.; Basu, S. Radiotracer study of synergic effect of trioctyl phosphine oxide on the solvent extraction of gold (III)-β-diketonates. *J. Radioanal. Nucl. Chem.* **2012**, *292*, 131–139. [CrossRef]

113. Dey, P.; Basu, S. Radiotracer study of the effects of organophosphorus donors on the extraction of iron(III) with 2-hydroxy-N-phenylbenzamide in n-butanol. *Radiochemistry* **2011**, *53*, 370–374. [CrossRef]

114. Parent, M.; Cornelis, R.; Dams, R.; Alt, F. Investigation of extraction and back-extraction behaviour of platinum (IV) with rubeanic acid in tributyl phosphate, with tributyl phosphate and with thenoyltrifluoroacetone in n-butyl alcohol-acetophenone by means of platinum-191 radiotracer for platinum-enrichment purposes. *Anal. Chim. Acta* **1993**, *281*, 153–160. [CrossRef]

115. Rotuska, K.; Chmielewski, T. Growing role of solvent extraction in copper ores processing. *Physicochem. Probl. Miner. Process.* **2008**, *42*, 29–36.

116. Chmielewski, T. Hydrometallurgy in Kghm Polska Miedz SA—Circumstances, Needs and Perspectives of Application. *Sep. Sci. Technol.* **2012**, *47*, 1264–1277. [CrossRef]

117. Watling, H.R. Chalcopyrite hydrometallurgy at atmospheric pressure: 2. Review of acidic chloride process options. *Hydrometallurgy* **2014**, *146*, 96–110. [CrossRef]

118. Tunsu, C.; Lapp, J.B.; Ekberg, C.; Retegan, T. Selective separation of yttrium and europium using Cyanex 572 for applications in fluorescent lamp waste processing. *Hydrometallurgy* **2016**, *166*, 98–106. [CrossRef]

119. Ciacci, L.; Vassura, I.; Passarini, F. Shedding Light on the Anthropogenic Europium Cycle in the EU–28. Marking Product Turnover and Energy Progress in the Lighting Sector. *Resources* **2018**, *7*, 59. [CrossRef]

120. Preston, J.S.; Preez, A.C.D. The solvent extraction of europium (II) by some organophosphorus and carboxylic acids. *Solvent Extr. Ion Exch.* **1991**, *9*, 237–257. [CrossRef]

121. Saad, E.A.; El-Atrash, A.M. Thermodynamics of the extraction of europium (III) radiotracer by benzyl-phosphonic acid monoester. *J. Radioanal. Nucl. Chem. Artic.* **1989**, *134*, 415–421. [CrossRef]

122. Ghani, L.; Shahida, S.; Ali, A.; Khan, M.H.; Aziz, B.; Masood, M.; Badshah, S.L.; Khan, M. Liquid–liquid extraction of Eu(lll) using synergic mixture of 1-phenyl-3-methyl-4-trifluoroacetyl-2-pyrazolin-5-one and crown ethers. *SN Appl. Sci.* **2020**, *2*, 1–10. [CrossRef]

123. Rim, K.T.; Koo, K.H.; Park, J.S. Toxicological Evaluations of Rare Earths and Their Health Impacts to Workers: A Literature Review. *Saf. Health Work.* **2013**, *4*, 12–26. [CrossRef] [PubMed]

124. Kumar, V.; Luo, Z. A Review on X-ray Excited Emission Decay Dynamics in Inorganic Scintillator Materials. *Photonics* **2021**, *8*, 71. [CrossRef]

125. Lin, Y.; Wu, H.; Smart, N.G.; Wai, C.M. Studies on in-situ chelation/supercritical fluid extraction of lanthanides and actinides using a radiotracer technique. *Sep. Sci. Technol.* **2001**, *36*, 1149–1162. [CrossRef]

126. Regueiro, M.; Alonso-Jimenez, A. Minerals in the future of Europe. *Miner. Econ.* **2021**, *34*, 209–224. [CrossRef]

127. Schmidt, M. Scarcity and Environmental Impact of Mineral Resources—An Old and Never-Ending Discussion. *Resources* **2019**, *8*, 2. [CrossRef]

128. Burlakovs, J.; Vincevica-Gaile, Z.; Krievans, M.; Jani, Y.; Horttanainen, M.; Pehme, K.M.; Dace, E.; Setyobudi, R.H.; Pilecka, J.; Denafas, G.; et al. Platinum Group Elements in Geosphere and Anthroposphere: Interplay among the Global Reserves, Urban Ores, Markets and Circular Economy. *Minerals* **2020**, *10*, 558. [CrossRef]

129. Hughes, A.E.; Haque, N.; Northey, S.A.; Giddey, S. Platinum Group Metals: A Review of Resources, Production and Usage with a Focus on Catalysts. *Resources* **2021**, *10*, 93. [CrossRef]

130. Xu, B.; Chen, Y.; Zhou, Y.; Zhang, B.; Liu, G.; Li, Q.; Yang, Y.; Jiang, T. A Review of Recovery of Palladium from the Spent Automobile Catalysts. *Metals* **2022**, *12*, 533. [CrossRef]

131. Eccles, S.F. Gamma ray spectroscopy of 107Cd, 109Pd and 111Pd. *Physica* **1962**, *28*, 251–261. [CrossRef]

132. Nichols, A.L. Comments on evaluation Pd-Comments on evaluation of decay data A.1. *Eval. Proced.* 2009; pp. 1–10. Available online: http://www.lnhb.fr/nuclides/Pd-109_com.pdf (accessed on 10 March 2022).

133. Jiang, J.; Liu, C.; Zhou, W.; Gao, H. The extraction of low-concentrations of gold(I) with 198Au as a radiotracer. *J. Radioanal. Nucl. Chem.* **2002**, *254*, 405–408. [CrossRef]

134. Tom, H.; Henrik, S.; Kari, A.A. *Minerals for The Green Economy. Trondheim, Norway*. 2017; pp. 1–15. Available online: https://www.ngu.no/sites/default/files/Minerals%20for%20the%20green%20economy%202016_screen.pdf (accessed on 3 February 2022).

135. Hagelüken, C.; Goldmann, D. Recycling and circular economy—Towards a closed loop for metals in emerging clean technologies. *Miner. Econ.* **2022**, *1*, 1–24. [CrossRef]

136. Billah, A.A.; Pujiyanto, A.; Hambali, H.; Lestari, E. Recovery of Gold from Radioactive Gold Waste Using the Redox Replacement Method with Zn-Foil Reductor. *IOP Conf. Ser. Mater. Sci. Eng.* **2019**, *546*, 022002. [CrossRef]

137. Dey, P.; Banerjee, S.; Basu, S. Radiotracer study of synergistic effects of neutral donors on the extraction of gold with N-(Thioacetyl)benzamide in chloroform. *Radiochemistry* **2012**, *54*, 153–158. [CrossRef]

138. Jiang, J.; Zhou, W.; Gao, H.; Wu, J.; Xu, G. Solvent extraction and stripping of gold (I) cyanide in the tetradecyldimethylbenzylammonium chloride system. *Hydrometallurgy* **2003**, *70*, 73–81. [CrossRef]

139. Jiang, J.; Wang, X.; Zhou, W.; Gao, H.; Wu, J. Extraction of gold from alkaline cyanide solution by the tetradecyldimethylbenzylammonium chloride/tri-n-butyl phosphate/n-heptane system based on a. *Phys. Chem. Chem. Phys.* **2002**, *4*, 4489–4494. Available online: https://pubs.rsc.org/en/content/articlehtml/2002/cp/b203467k (accessed on 1 December 2022). [CrossRef]

140. Mandal, M.; Sarkar, R.; Basu, S. Determination of solubility parameters of cobalt (II) and indium (III) oxinates by tracer technique. *Radiochim. Acta* **2009**, *97*, 759–762. [CrossRef]

141. Wang, K.; Pei, P.; Zuo, Y.; Wei, M.; Wang, H.; Zhang, P.; Chen, Z.; Shang, N. Magnetic zinc-air batteries for storing wind and solar energy. *IScience* **2022**, *25*, 103837. [CrossRef]

142. Lerum, H.V.; Sand, S.; Eriksen, D.Ø.; Wibetoe, G.; Omtvedt, J.P. Comparison of single-phase and two-phase measurements in extraction, separation and back-extraction of Cd, Zn and Co from a multi-element matrix using Aliquat 336. *J. Radioanal. Nucl. Chem.* **2020**, *324*, 1203–1214. [CrossRef]

143. Sokolov, A.; Valeev, D.; Kasikov, A. Solvent extraction of iron (III) from Al chloride solution of bauxite HCl leaching by mixture of aliphatic alcohol and ketone. *Metals* **2021**, *11*, 321. [CrossRef]

144. Grimsley, L.F. Iron and Cobalt. *Patty's Toxicol.* **2021**, 647. [CrossRef]

145. Mishra, S.P.; Singh, V.K. Radiotracer technique in adsorption study—XIII. Adsorption of barium and strontium ions on chromium (IV) oxide powder. *Appl. Radiat. Isot.* **1995**, *46*, 847–853. [CrossRef]

146. Gujar, R.B.; Mohapatra, P.K.; Iqbal, M.; Huskens, J.; Verboom, W. Selective uptake of thorium(IV) from nitric acid medium using two extraction chromatographic resins based on diglycolamide-calix[4]arenes: Application to thorium-uranyl separation in an actual sample. *J. Chromatogr. A* **2021**, *1653*, 1–9. [CrossRef] [PubMed]

147. Baybaş, D.; Ulusoy, U. Polyacrylamide-clinoptilolite/Y-zeolite composites: Characterization and adsorptive features for terbium. *J. Hazard. Mater.* **2011**, *187*, 241–249. [CrossRef] [PubMed]

148. Dubey, S.S.; Battula, R. Removal of cerium ions from aqueous solution by hydrous ferric oxide–A radiotracer study. *J. Hazard. Mater.* **2011**, *186*, 1028–1032. Available online: https://www.sciencedirect.com/science/article/pii/S0304389410015116 (accessed on 29 September 2022). [CrossRef] [PubMed]

149. Johnson, B.E.; Santschi, P.H.; Chuang, C.Y.; Otosaka, S.; Addleman, R.S.; Douglas, M.; Rutledge, R.D.; Chouyyok, W.; Davidson, J.D.; Fryxell, G.E.; et al. Collection of lanthanides and actinides from natural waters with conventional and nanoporous sorbents. *Environ. Sci. Technol.* **2012**, *46*, 11251–11258. [CrossRef]

150. Bertelsen, E.; Deodhar, G.; Kluherz, K.T.; Davidson, M.; Adams, M.L.; Trewyn, B.G.; Shafer, J.C. Microcolumn lanthanide separation using bis-(2-ethylhexyl) phosphoric acid functionalized ordered mesoporous carbon materials. *J. Chromatogr. A* **2019**, *1595*, 248–256. [CrossRef] [PubMed]

151. Symeopoulos, B.; Soupioni, M.; Misaelides, P.; Godelitsas, A.; Barbayiannis, N. Neodymium sorption by clay minerals and zeoliferous rocks. *J. Radioanal. Nucl. Chem.* **1996**, *212*, 421–429. [CrossRef]

152. Xiangke, W.; Wenming, D.; Xiongxin, D.; Aixia, W.; Jinzhou, D.; Zuyi, T. Sorption and desorption of Eu and Yb on alumina: Mechanisms and effect of fulvic acid. *Appl. Radiat. Isot.* **2000**, *52*, 165–173. [CrossRef]

153. Ansari, S.A.; Mohapatra, P.K.; Iqbal, M.; Huskens, J.; Verboom, W. Sorption of americium(III) and europium(III) from nitric acid solutions by a novel diglycolamide-grafted silica-based resins: Part 2. Sorption isotherms, column and radiolytic stability studies. *Radiochim. Acta* **2014**, *102*, 903–910. [CrossRef]

154. Koeppenkastrop, D.; de Carlo, E.H. Uptake of Rare Earth Elements from Solution by Metal Oxides. *Environ. Sci. Technol.* **1993**, *27*, 1796–1802. [CrossRef]

155. Snow, M.; Ward, J. Fundamental distribution coefficient data and separations using eichrom extraction chromatographic resins. *J. Chromatogr. A* **2020**, *1620*, 460833. [CrossRef] [PubMed]

156. Dietz, M.; Horwitz, E.P.; Sajdak, L.R.; Renato, C. An improved extraction chromatographic resin for the separation of uranium from acidic nitrate media. *Talanta* **2001**, *54*, 1173–1184. [CrossRef] [PubMed]

157. Momen, M.A.; Healy, M.R.; Tsouris, C.; Jansone-Popova, S.; Depaoli, D.W.; Moyer, B.A. Extraction Chromatographic Materials for Clean Hydrometallurgical Separation of Rare-Earth Elements Using Diglycolamide Extractants. *Ind. Eng. Chem. Res.* **2019**, *58*, 20081–20089. [CrossRef]

158. Momen, M.A.; Dietz, M.L. High-capacity extraction chromatographic materials based on polysulfone microcapsules for the separation and preconcentration of lanthanides from aqueous solution. *Talanta* **2019**, *197*, 612–621. [CrossRef] [PubMed]

159. Khalifa, S.M.; Raieh, M.; El-Dessouky, M.; Aly, H.F. Extraction chromatography of some metal radiotracers using adogen-381 HCl and KSCN systems. *Chromatographia* **1982**, *15*, 315–317. [CrossRef]

160. Devi, P.S.R.; Joshi, S.; Verma, R.; Reddy, A.V.R.; Lali, A.M.; Gantayet, L.M. Ion-exchange separation of 60Co and 125Sb from zirconium for radioactive waste management. *Nucl. Technol.* **2010**, *171*, 220–227. [CrossRef]

161. Mandal, M.; Dhara, S.; Basu, S. Separation of Carrier-Free 115mIn from Its Parent 115Cd Using the Synthesized TODGA-Impregnated Silica Gel. *Radiochemistry* **2018**, *60*, 548–551. [CrossRef]

162. Ng, Q.K.T.; Olariu, C.I.; Yaffee, M.; Taelman, V.F.; Marincek, N.; Krause, T.; Meier, L.; Walter, M.A. Indium-111 labeled gold nanoparticles for in-vivo molecular targeting. *Biomaterials* **2014**, *35*, 7050–7057. [CrossRef]

163. Mandal, M.; Majumdar, D. Radiotracer studies for the uptake of silver from aqueous solution by TODGA-impregnated silica gel. *Radiochemistry* **2015**, *57*, 417–420. [CrossRef]

164. Greenberg, R.R.; Bode, P.; de Nadai Fernandes, E.A. Neutron activation analysis: A primary method of measurement. *Spectrochim. Acta Part B* **2011**, *66*, 193–241. [CrossRef]

165. Coler, D. The 5 Most Common Ways to Prepare Samples for XRF Analysis. Available online: https://www.armi.com/blog/the-5-most-common-ways-to-prepare-samples-for-xrf-analysis (accessed on 24 May 2017).

166. Duchesne, J.; Belgica, G.B. XRF major and trace element determination in Fe-Ti oxide minerals. *Orbi. Uliege. Be* **2009**, *12*, 205–212. Available online: https://orbi.uliege.be/bitstream/2268/6194/1/VOL%2012%20PART%203-4%20DUCHESNE%20205-212.pdf (accessed on 1 December 2022).